

The Lehigh River, White Haven, Pennsylvania.
Open channel flows are everywhere, often rough
and turbulent, as in this photo. They are analyzed
by the methods of the present chapter. (*Courtesy of
Dr. E. R. Degginger/Color-Pic Inc.*)

Chapter 10

Open-Channel Flow

Motivation. The duct flows of Chap. 6 were driven by a pressure difference between the ends of the duct. Such channels are closed and full of fluid, either gas or liquid. By contrast, an *open-channel flow* is liquid only and is *not* full; i.e., there is always a free surface exposed to ambient pressure. The basic balance of forces is between gravity (fluid weight) and friction.

Practical open-channel problems almost always concern *water* as the relevant fluid. The flow is generally turbulent, due to its large scale and small kinematic viscosity, and is three-dimensional, sometimes unsteady, and often surprisingly complex due to geometric effects. This chapter presents some simple engineering theories and correlations for steady flow in straight channels of simple geometry. Many of the concepts from steady duct flow—hydraulic diameter, friction factor, head losses—apply also to open channels.

10.1 Introduction

Simply stated, open-channel flow is the flow of a liquid in a conduit with a free surface. There are many practical examples, both artificial (flumes, spillways, canals, weirs, drainage ditches, culverts) and natural (streams, rivers, estuaries, floodplains). This chapter introduces the elementary analysis of such flows, which are dominated by the effects of gravity.

The presence of the free surface, which is essentially at atmospheric pressure, both helps and hurts the analysis. It helps because the pressure can be taken constant along the free surface, which therefore is equivalent to the *hydraulic grade line* (HGL) of the flow. Unlike flow in closed ducts, the pressure gradient is not a direct factor in open-channel flow, where the balance of forces is confined to gravity and friction.¹ But the free surface complicates the analysis because its shape is a priori unknown: The depth profile changes with conditions and must be computed as part of the problem, especially in unsteady problems involving wave motion.

Before proceeding, we remark, as usual, that whole books have been written on open-channel hydraulics [1 to 4]. There are also specialized texts devoted to wave motion [5 to 7] and to engineering aspects of coastal free-surface flows [8, 9]. This chapter is only an introduction to broader and more detailed treatments.

¹Surface tension is rarely important because open channels are normally quite large and have a very large Weber number.

The One-Dimensional Approximation

An open channel always has two sides and a bottom, where the flow satisfies the no-slip condition. Therefore even a straight channel has a three-dimensional velocity distribution. Some measurements of straight-channel velocity contours are shown in Fig. 10.1. The profiles are quite complex, with maximum velocity typically occurring in the midplane about 20 percent below the surface. In very broad shallow channels the maximum velocity is near the surface, and the velocity profile is nearly logarithmic from the bottom to the free surface, as in Eq. (6.84). In noncircular channels there are also secondary motions similar to Fig. 6.16 for closed-duct flows. If the channel curves or meanders, the secondary motion intensifies due to centrifugal effects, with high velocity occurring near the outer radius of the bend. Curved natural channels are subject to strong bottom erosion and deposition effects.

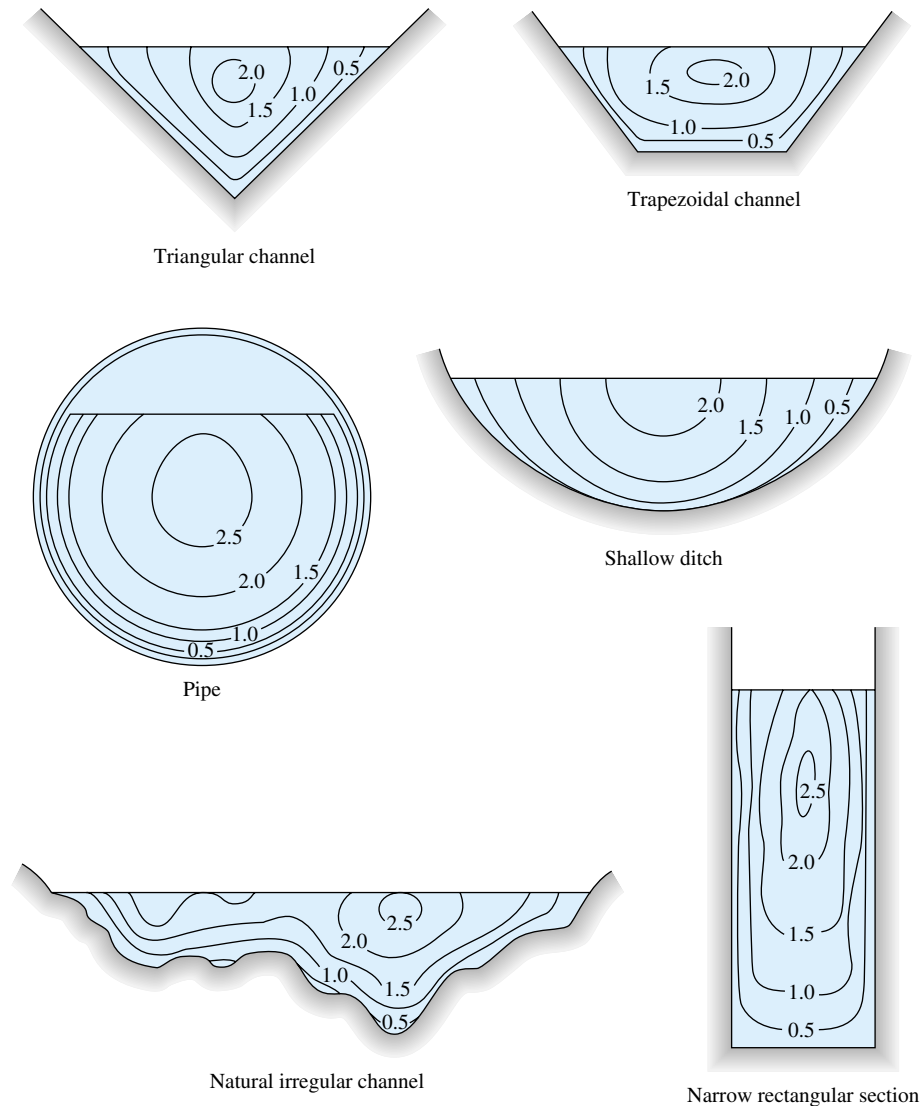
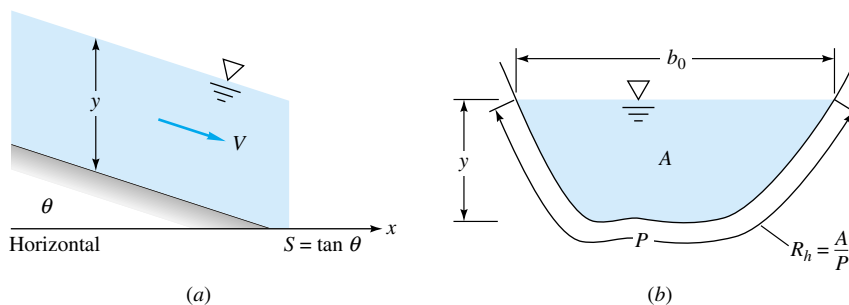


Fig. 10.1 Measured isovelocity contours in typical straight open-channel flows. (From Ref. 3.)

Fig. 10.2 Geometry and notation for open-channel flow: (a) side view; (b) cross section. All these parameters are constant in uniform flow.



With the advent of the supercomputer, it is possible to make numerical simulations of complex flow patterns such as in Fig. 10.1 [23]. However, the practical engineering approach, used here, is to make a one-dimensional-flow approximation, as in Fig. 10.2. Since the liquid density is nearly constant, the steady-flow continuity equation reduces to constant-volume flow Q along the channel

$$Q = V(x)A(x) = \text{const} \quad (10.1)$$

where V is average velocity and A the local cross-sectional area, as sketched in Fig. 10.2.

A second one-dimensional relation between velocity and channel geometry is the energy equation, including friction losses. If points 1 (upstream) and 2 (downstream) are on the free surface, $p_1 = p_2 = p_a$, and we have, for steady flow,

$$\frac{V_1^2}{2g} + z_1 = \frac{V_2^2}{2g} + z_2 + h_f \quad (10.2)$$

where z denotes the total elevation of the free surface, which includes the water depth y (see Fig. 10.2a) plus the height of the (sloping) bottom. The friction head loss h_f is analogous to head loss in duct flow from Eq. (6.30):

$$h_f \approx f \frac{x_2 - x_1}{D_h} \frac{V_{\text{av}}^2}{2g} \quad D_h = \text{hydraulic diameter} = \frac{4A}{P} \quad (10.3)$$

where f is the average friction factor (Fig. 6.13) between sections 1 and 2. Since channels are irregular in shape, their “size” is taken to be the hydraulic diameter, with P the *wetted* perimeter—see Fig. 10.2b. Actually, open-channel formulas typically use the *hydraulic radius*

$$R_h = \frac{1}{4} D_h = \frac{A}{P} \quad (10.4)$$

The local Reynolds number of the channel would be $\text{Re} = VD_h/\nu$, which is usually highly turbulent ($>1 \text{ E}5$). The only commonly occurring laminar channel flows are the thin sheets which form as rainwater drains from crowned streets and airport runways.

The wetted perimeter P (see Fig. 10.2b) includes the sides and bottom of the channel but not the free surface and, of course, not the parts of the sides above the water level. For example, if a rectangular channel is b wide and h high and contains water to depth y , its wetted perimeter is

$$P = b + 2y \quad (10.5)$$

not $2b + 2h$.

Although the Moody chart (Fig. 6.13) would give a good estimate of the friction factor in channel flow, in practice it is seldom used. An alternate correlation due to Robert Manning, discussed in Sec. 10.2, is the formula of choice in open-channel hydraulics.

Flow Classification by Depth Variation

The most common method of classifying open-channel flows is by the rate of change of the free-surface depth. The simplest and most widely analyzed case is *uniform flow*, where the depth (hence the velocity in steady flow) remains constant. Uniform-flow conditions are approximated by long straight runs of constant-slope and constant-area channel. A channel in uniform flow is said to be moving at its *normal depth* y_n , which is an important design parameter.

If the channel slope or cross section changes or there is an obstruction in the flow, then the depth changes and the flow is said to be *varied*. The flow is *gradually varying* if the one-dimensional approximation is valid and *rapidly varying* if not. Some examples of this method of classification are shown in Fig. 10.3. The classes can be summarized as follows:

1. Uniform flow (constant depth and slope)
2. Varied flow
 - a. Gradually varied (one-dimensional)
 - b. Rapidly varied (multidimensional)

Typically uniform flow is separated from rapidly varying flow by a region of gradually varied flow. Gradually varied flow can be analyzed by a first-order differential equation (Sec. 10.6), but rapidly varying flow usually requires experimentation or three-dimensional potential theory.

Flow Classification by Froude Number: Surface Wave Speed

A second and very interesting classification is by dimensionless Froude number, which for a rectangular or very wide channel takes the form $Fr = V/(gy)^{1/2}$, where y is the

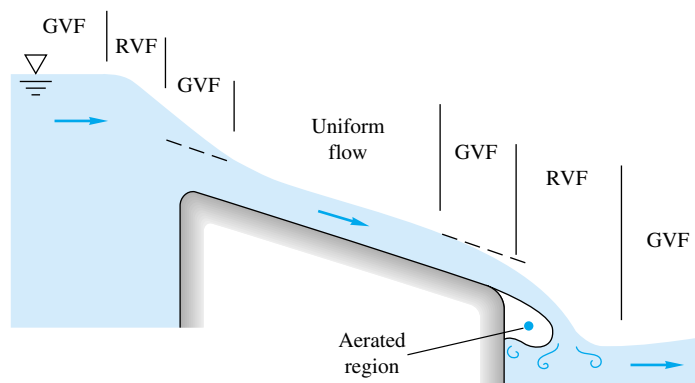


Fig. 10.3 Open-channel flow classified by regions of rapidly varying flow (RVF), gradually varying flow (GVF), and uniform-flow depth profiles.

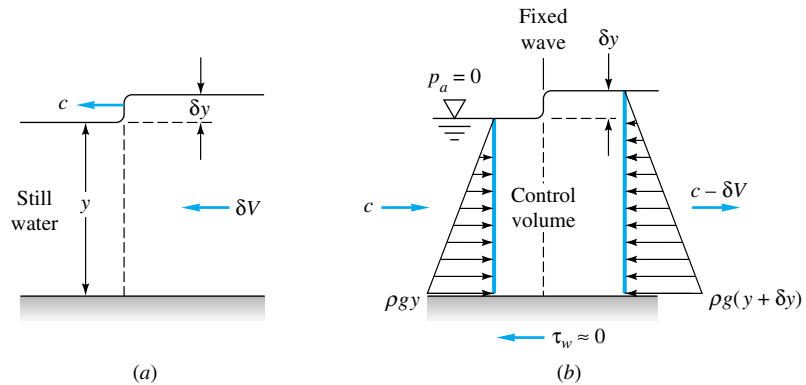


Fig. 10.4 Analysis of a small surface wave propagating into still shallow water; (a) moving wave, nonsteady frame; (b) fixed wave, inertial frame of reference.

water depth. The three flow regimes are

$$\begin{aligned}
 \text{Fr} < 1.0 & \quad \text{subcritical flow} \\
 \text{Fr} = 1.0 & \quad \text{critical flow} \\
 \text{Fr} > 1.0 & \quad \text{supercritical flow}
 \end{aligned}
 \tag{10.6}$$

The Froude number for irregular channels is defined in Sec. 10.4. As mentioned in Sec. 9.10, there is a strong analogy here with the three compressible-flow regimes of the Mach number: subsonic ($\text{Ma} < 1$), sonic ($\text{Ma} = 1$), and supersonic ($\text{Ma} > 1$). We shall pursue the analogy in Sec. 10.4.

The Froude-number denominator $(gy)^{1/2}$ is the speed of an infinitesimal shallow-water surface wave. We can derive this with reference to Fig. 10.4a, which shows a wave of height δy propagating at speed c into still liquid. To achieve a steady-flow inertial frame of reference, we fix the coordinates on the wave as in Fig. 10.4b, so that the still water moves to the right at velocity c . Figure 10.4 is exactly analogous to Fig. 9.1, which analyzed the speed of sound in a fluid.

For the control volume of Fig. 10.4b, the one-dimensional continuity relation is, for channel width b ,

$$\rho c y b = \rho (c - \delta V)(y + \delta y)b$$

$$\text{or} \quad \delta V = c \frac{\delta y}{y + \delta y} \tag{10.7}$$

This is analogous to Eq. (9.10); the velocity change δV induced by a surface wave is small if the wave is “weak,” $\delta y \ll y$. If we neglect bottom friction in the short distance across the wave in Fig. 10.4b, the momentum relation is a balance between the net hydrostatic pressure force and momentum

$$-\frac{1}{2}\rho g b [(y + \delta y)^2 - y^2] = \rho c b y (c - \delta V - c)$$

$$\text{or} \quad g \left(1 + \frac{\frac{1}{2} \delta y}{y} \right) \delta y = c \delta V \tag{10.8}$$

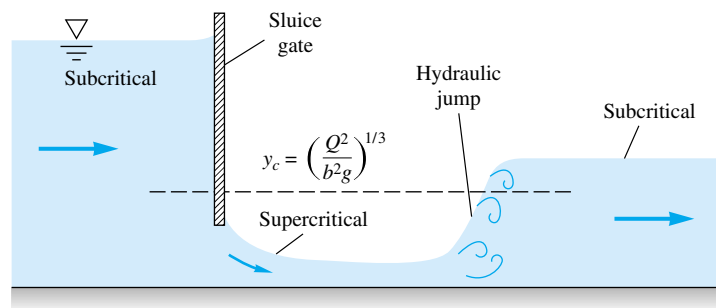


Fig. 10.5 Flow under a sluice gate accelerates from subcritical to critical to supercritical flow and then jumps back to subcritical flow.

This is analogous to Eq. (9.12). By eliminating δV between Eqs. (10.7) and (10.8) we obtain the desired expression for wave propagation speed

$$c^2 = gy \left(1 + \frac{\delta y}{y}\right) \left(1 + \frac{1}{2} \frac{\delta y}{y}\right) \quad (10.9)$$

The “stronger” the wave height δy , the faster the wave speed c , by analogy with Eq. (9.13). In the limit of an infinitesimal wave height $\delta y \rightarrow 0$, the speed becomes

$$c_0^2 = gy \quad (10.10)$$

This is the surface-wave equivalent of fluid sound speed a , and thus the Froude number in channel flow $Fr = V/c_0$ is the analog of the Mach number.

As in gas dynamics, a channel flow can accelerate from subcritical to critical to supercritical flow and then return to subcritical flow through a sort of normal shock called a *hydraulic jump* (Sec. 10.5). This is illustrated in Fig. 10.5. The flow upstream of the sluice gate is subcritical. It then accelerates to critical and supercritical flow as it passes under the gate, which serves as a sort of “nozzle.” Further downstream the flow “shocks” back to subcritical flow because the downstream “receiver” height is too high to maintain supercritical flow. Note the similarity with the nozzle gas flows of Fig. 9.12.

The critical depth $y_c = [Q^2/(b^2g)]^{1/3}$ is sketched as a dashed line in Fig. 10.5 for reference. Like the normal depth y_n , y_c is an important parameter in characterizing open-channel flow (see Sec. 10.4).

An excellent discussion of the various regimes of open-channel flow is given in Ref. 10.

10.2 Uniform Flow; the Chézy Formula

Uniform flow can occur in long straight runs of constant slope and constant channel cross section. The water depth is constant at $y = y_n$, and the velocity is constant at $V = V_0$. Let the slope be $S_0 = \tan \theta$, where θ is the angle the bottom makes with the horizontal, considered positive for downhill flow. Then Eq. (10.2), with $V_1 = V_2 = V_0$, becomes

$$h_f = z_1 - z_2 = S_0 L \quad (10.11)$$

where L is the horizontal distance between sections 1 and 2. The head loss thus balances the loss in height of the channel. The flow is essentially fully developed, so that the Darcy-Weisbach relation, Eq. (6.30), holds

$$h_f = f \frac{L}{D_h} \frac{V_0^2}{2g} \quad D_h = 4R_h \quad (10.12)$$

with $D_h = 4A/P$ used to accommodate noncircular channels. The geometry and notation for open-channel flow analysis are shown in Fig. 10.2.

By combining Eqs. (10.11) and (10.12) we obtain an expression for flow velocity in uniform channel flow

$$V_0 = \left(\frac{8g}{f}\right)^{1/2} R_h^{1/2} S_0^{1/2} \quad (10.13)$$

For a given channel shape and bottom roughness, the quantity $(8g/f)^{1/2}$ is constant and can be denoted by C . Equation (10.13) becomes

$$V_0 = C(R_h S_0)^{1/2} \quad Q = CA(R_h S_0)^{1/2} \quad (10.14)$$

These are called the *Chézy formulas*, first developed by the French engineer Antoine Chézy in conjunction with his experiments on the Seine River and the Courpalet Canal in 1769. The quantity C , called the *Chézy coefficient*, varies from about 60 ft^{1/2}/s for small rough channels to 160 ft^{1/2}/s for large smooth channels (30 to 90 m^{1/2}/s in SI units).

Over the past century a great deal of hydraulics research [11] has been devoted to the correlation of the Chézy coefficient with the roughness, shape, and slope of various open channels. Correlations are due to Ganguillet and Kutter in 1869, Manning in 1889, Bazin in 1897, and Powell in 1950 [11]. All these formulations are discussed in delicious detail in Ref. 3, chap. 5. Here we confine our treatment to Manning's correlation, the most popular.

The Manning Roughness Correlation

The most fundamentally sound approach to the Chézy formula is to use Eq. (10.13) with f estimated from the Moody friction-factor chart, Fig. 6.13. Indeed, the open channel research establishment [17] strongly recommends use of the friction factor in all calculations. Since typical channels are large and rough, we would generally use the fully rough turbulent-flow limit of Eq. (6.64):

$$f \approx \left(2.0 \log \frac{14.8R_h}{\epsilon}\right)^{-2} \quad (10.15a)$$

A special case, for rocky channel beds, is recommended in Ref. 2:

$$f \approx \left[1.2 + 2.03 \log \left(\frac{R_h}{d_{84\%}}\right)\right]^{-2} \quad (10.15b)$$

where $d_{84\%}$ is the size for which 84 percent of the rocks are smaller (the largest rocks dominate the friction in the channel). Note that $d_{84\%}$ and ϵ are *not* equal, ϵ being an overall average size. In spite of the attractiveness of this friction-factor approach, most engineers prefer to use a simple (dimensional) correlation published in 1891 by Robert Manning [12], an Irish engineer. In tests with real channels, Manning found that the Chézy coefficient C increased approximately as the sixth root of the channel size. He proposed the simple formula

$$C = \left(\frac{8g}{f}\right)^{1/2} \approx \alpha \frac{R_h^{1/6}}{n} \quad (10.16)$$

where n is a roughness parameter. Since the formula is clearly not dimensionally consistent, it requires a conversion factor α which changes with the system of units used:

$$\alpha = 1.0 \quad \text{SI units} \quad \alpha = 1.486 \quad \text{BG units} \quad (10.17)$$

Recall that we warned about this awkwardness in Example 1.4. You may verify that α is the cube root of the conversion factor between the meter and your chosen length scale: In BG units, $\alpha = (3.2808 \text{ ft/m})^{1/3} = 1.486$.*

The Manning formula for uniform-flow velocity is thus

$$\begin{aligned} V_0 \text{ (m/s)} &\approx \frac{1.0}{n} [R_h \text{ (m)}]^{2/3} S_0^{1/2} \\ V_0 \text{ (ft/s)} &\approx \frac{1.486}{n} [R_h \text{ (ft)}]^{2/3} S_0^{1/2} \end{aligned} \quad (10.18)$$

The channel slope S_0 is dimensionless, and n is taken to be the same in both systems. The volume flow rate simply multiplies this result by the area:

$$\text{Uniform flow:} \quad Q = V_0 A \approx \frac{\alpha}{n} A R_h^{2/3} S_0^{1/2} \quad (10.19)$$

Experimental values of n (and the corresponding roughness height) are listed in Table 10.1 for various channel surfaces. There is a factor-of-15 variation from a smooth glass surface ($n \approx 0.01$) to a tree-lined floodplain ($n \approx 0.15$). Due to the irregularity of typical channel shapes and roughness, the scatter bands in Table 10.1 should be taken seriously.

Since Manning's sixth-root size variation is not exact, real channels can have a variable n depending upon the water depth. The Mississippi River near Memphis, Tennessee, has $n \approx 0.032$ at 40-ft flood depth, 0.030 at normal 20-ft depth, and 0.040 at 5-ft low-stage depth. Seasonal vegetative growth and factors such as bottom erosion can also affect the value of n .

EXAMPLE 10.1

A finished-concrete 8-ft-wide rectangular channel has a bed slope of 0.5° and a water depth of 4 ft. Predict the uniform flow rate in ft^3/s .

Solution

Part (a) From Table 10.1, for finished concrete, $n \approx 0.012$. The slope $S_0 = \tan 0.5^\circ = 0.00873$. For depth $y = 4$ ft and width $b = 8$ ft, the geometric properties are

$$A = by = (8 \text{ ft})(4 \text{ ft}) = 32 \text{ ft}^2 \quad P = b + 2y = 8 + 2(4) = 16 \text{ ft}$$

$$R_h = \frac{A}{P} = \frac{32 \text{ ft}^2}{16 \text{ ft}} = 2.0 \text{ ft} \quad D_h = 4R_h = 8.0 \text{ ft}$$

From Manning's formula (10.19) in BG units, the estimated flow rate is

$$Q \approx \frac{1.486}{n} A R_h^{2/3} S_0^{1/2} = \frac{1.486}{0.012} (32 \text{ ft}^2)(2.0 \text{ ft})^{2/3}(0.00873)^{1/2} \approx 590 \text{ ft}^3/\text{s} \quad \text{Ans.}$$

*An interesting discussion of the history and "dimensionality" of Manning's formula is given in Ref. 3, pp. 98–99.

Table 10.1 Experimental Values of Manning's n Factor*

	n	Average roughness height ϵ	
		ft	mm
Artificial lined channels:			
Glass	0.010 \pm 0.002	0.0011	0.3
Brass	0.011 \pm 0.002	0.0019	0.6
Steel, smooth	0.012 \pm 0.002	0.0032	1.0
Painted	0.014 \pm 0.003	0.0080	2.4
Riveted	0.015 \pm 0.002	0.012	3.7
Cast iron	0.013 \pm 0.003	0.0051	1.6
Cement, finished	0.012 \pm 0.002	0.0032	1.0
Unfinished	0.014 \pm 0.002	0.0080	2.4
Planed wood	0.012 \pm 0.002	0.0032	1.0
Clay tile	0.014 \pm 0.003	0.0080	2.4
Brickwork	0.015 \pm 0.002	0.012	3.7
Asphalt	0.016 \pm 0.003	0.018	5.4
Corrugated metal	0.022 \pm 0.005	0.12	37
Rubble masonry	0.025 \pm 0.005	0.26	80
Excavated earth channels:			
Clean	0.022 \pm 0.004	0.12	37
Gravelly	0.025 \pm 0.005	0.26	80
Weedy	0.030 \pm 0.005	0.8	240
Stony, cobbles	0.035 \pm 0.010	1.5	500
Natural channels:			
Clean and straight	0.030 \pm 0.005	0.8	240
Sluggish, deep pools	0.040 \pm 0.010	3	900
Major rivers	0.035 \pm 0.010	1.5	500
Floodplains:			
Pasture, farmland	0.035 \pm 0.010	1.5	500
Light brush	0.05 \pm 0.02	6	2000
Heavy brush	0.075 \pm 0.025	15	5000
Trees	0.15 \pm 0.05	?	?

*A more complete list is given in Ref. 3, pp. 110–113.

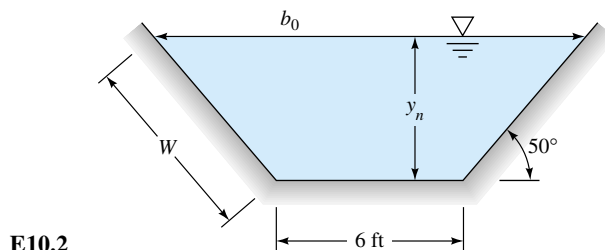
Considering the uncertainty in n (± 17 percent), it would be more realistic to report this estimate as $Q \approx 600 \pm 100 \text{ ft}^3/\text{s}$. An alternate estimate, using the Moody formula (10.15) with $\epsilon = 0.0032 \text{ ft}$ from Table 10.1, would give $Q \approx 540 \text{ ft}^3/\text{s}$.

Normal-Depth Estimates

With water depth y known, the computation of Q in Example 10.1 was quite straightforward. However, if Q is given, the computation of the normal depth y_n may require iteration or trial and error. Since the normal depth is a characteristic flow parameter, this is an important type of problem.

EXAMPLE 10.2

The asphalt-lined trapezoidal channel in Fig. E10.2 carries $300 \text{ ft}^3/\text{s}$ of water under uniform-flow conditions when $S = 0.0015$. What is the normal depth y_n ?



Solution

From Table 10.1, for asphalt, $n \approx 0.016$. The area and hydraulic radius are functions of y_n , which is unknown

$$b_0 = 6 \text{ ft} + 2y_n \cot 50^\circ \quad A = \frac{1}{2}(6 + b_0)y_n = 6y_n + y_n^2 \cot 50^\circ$$

$$P = 6 + 2W = 6 + 2y_n \csc 50^\circ$$

From Manning's formula (10.19) with a known $Q = 300 \text{ ft}^3/\text{s}$, we have

$$300 = \frac{1.49}{0.016} (6y_n + y_n^2 \cot 50^\circ) \left(\frac{6y_n + y_n^2 \cot 50^\circ}{6 + 2y_n \csc 50^\circ} \right)^{2/3} (0.0015)^{1/2}$$

or
$$(6y_n + y_n^2 \cot 50^\circ)^{5/3} = 83.2(6 + 2y_n \csc 50^\circ)^{2/3}$$

One can iterate this formula laboriously and eventually find $y_n \approx 4.6 \text{ ft}$. However, it is a perfect candidate for EES. Instead of manipulating and programming the final formula, one might simply evaluate each separate part of the Chézy equation (in English units, with angles in degrees):

```
P = 6 + 2*yn/sin(50)
A = 6*yn + yn^2/tan(50)
Rh = A/P
300 = 1.49/0.016*A*Rh^(2/3)*0.0015^0.5
```

Hit Solve from the menu bar and EES complains of “negative numbers to a power”. Go back to Variable Information on the menu bar and make sure that y_n is positive. EES then immediately solves for

$$P = 17.95 \quad A = 45.04 \quad R_h = 2.509 \quad y_n = 4.577 \text{ ft} \quad \text{Ans.}$$

Generally, EES is ideal for open-channel-flow problems where the depth is unknown.

Uniform Flow in a Partly Full Circular Pipe

Consider the partially full pipe of Fig. 10.6a in uniform flow. The maximum velocity and flow rate actually occur before the pipe is completely full. In terms of the pipe radius R and the angle θ up to the free surface, the geometric properties are

$$A = R^2 \left(\theta - \frac{\sin 2\theta}{2} \right) \quad P = 2R\theta \quad R_h = \frac{R}{2} \left(1 - \frac{\sin 2\theta}{2\theta} \right)$$

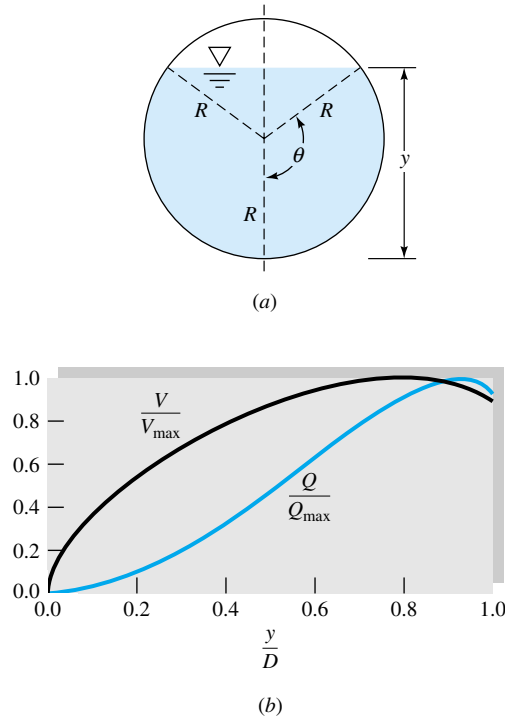


Fig. 10.6 Uniform flow in a partly full circular channel: (a) geometry; (b) velocity and flow rate versus depth.

The Manning formulas (10.19) predict a uniform flow as follows:

$$V_0 \approx \frac{\alpha}{n} \left[\frac{R}{2} \left(1 - \frac{\sin 2\theta}{2\theta} \right) \right]^{2/3} S_0^{1/2} \quad Q = V_0 R^2 \left(\theta - \frac{\sin 2\theta}{2} \right) \quad (10.20)$$

For a given n and slope S_0 , we may plot these two relations versus θ in Fig. 10.6*b*. There are two different maxima, as follows:

$$\begin{aligned} V_{\max} &= 0.718 \frac{\alpha}{n} R^{2/3} S_0^{1/2} & \text{at } \theta = 128.73^\circ & \text{ and } y = 0.813D \\ Q_{\max} &= 2.129 \frac{\alpha}{n} R^{8/3} S_0^{1/2} & \text{at } \theta = 151.21^\circ & \text{ and } y = 0.938D \end{aligned} \quad (10.21)$$

As shown in Fig. 10.6*b*, the maximum velocity is 14 percent more than the velocity when running full, and similarly the maximum discharge is 8 percent more. Since real pipes running nearly full tend to have somewhat unstable flow, these differences are not that significant.

10.3 Efficient Uniform-Flow Channels

The simplicity of Manning's formulation (10.19) enables us to analyze channel flows to determine the most efficient low-resistance sections for given conditions. The most common problem is that of maximizing R_h for a given flow area and discharge. Since $R_h = A/P$, maximizing R_h for given A is the same as minimizing the wetted perimeter

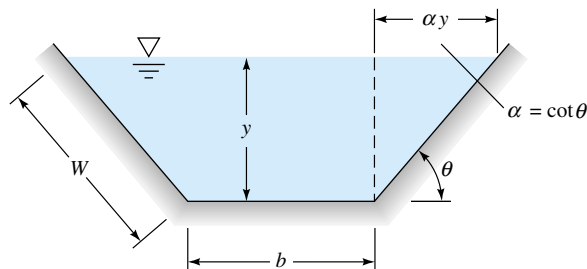


Fig. 10.7 Geometry of a trapezoidal channel section.

P. There is no general solution for arbitrary cross sections, but an analysis of the trapezoid section will show the basic results.

Consider the generalized trapezoid of angle θ in Fig. 10.7. For a given side angle θ , the flow area is

$$A = by + \alpha y^2 \quad \alpha = \cot \theta \quad (10.22)$$

The wetted perimeter is

$$P = b + 2W = b + 2y(1 + \alpha^2)^{1/2} \quad (10.23)$$

Eliminating b between (10.22) and (10.23) gives

$$P = \frac{A}{y} - \alpha y + 2y(1 + \alpha^2)^{1/2} \quad (10.24)$$

To minimize P , evaluate dP/dy for constant A and α and set equal to zero. The result is

$$A = y^2[2(1 + \alpha^2)^{1/2} - \alpha] \quad P = 4y(1 + \alpha^2)^{1/2} - 2\alpha y \quad R_h = \frac{1}{2}y \quad (10.25)$$

The last result is very interesting: For any angle θ , the most efficient cross section for uniform flow occurs when the hydraulic radius is half the depth.

Since a rectangle is a trapezoid with $\alpha = 0$, the most efficient rectangular section is such that

$$A = 2y^2 \quad P = 4y \quad R_h = \frac{1}{2}y \quad b = 2y \quad (10.26)$$

To find the correct depth y , these relations must be solved in conjunction with Manning's flow-rate formula (10.19) for the given discharge Q .

Best Trapezoid Angle

Equations (10.25) are valid for any value of α . What is the best value of α for a given depth and area? To answer this question, evaluate $dP/d\alpha$ from Eq. (10.24) with A and y held constant. The result is

$$2\alpha = (1 + \alpha^2)^{1/2} \quad \alpha = \cot \theta = \frac{1}{3^{1/2}}$$

$$\text{or} \quad \theta = 60^\circ \quad (10.27)$$

Thus the very best trapezoid section is half a hexagon.

Similar calculations with a circular channel section running partially full show best efficiency for a semicircle, $y = \frac{1}{2}D$. In fact, the semicircle is the best of all possible

channel sections (minimum wetted perimeter for a given flow area). The percentage improvement over, say, half a hexagon is very slight, however.

EXAMPLE 10.3

What are the best dimensions for a rectangular brick channel designed to carry $5 \text{ m}^3/\text{s}$ of water in uniform flow with $S_0 = 0.001$?

Solution

From Eq. (10.26), $A = 2y^2$ and $R_h = \frac{1}{2}y$. Manning's formula (10.19) in SI units gives, with $n \approx 0.015$ from Table 10.1,

$$Q = \frac{1.0}{n} AR_h^{2/3} S_0^{1/2} \quad \text{or} \quad 5 \text{ m}^3/\text{s} = \frac{1.0}{0.015} (2y^2) \left(\frac{1}{2}y\right)^{2/3} (0.001)^{1/2}$$

which can be solved for

$$y^{8/3} = 1.882 \text{ m}^{8/3}$$

$$y = 1.27 \text{ m} \quad \text{Ans.}$$

The proper area and width are

$$A = 2y^2 = 3.21 \text{ m}^2 \quad b = \frac{A}{y} = 2.53 \text{ m} \quad \text{Ans.}$$

It is constructive to see what flow rate a half-hexagon and semicircle would carry for the same area of 3.214 m^2 .

For the half-hexagon (HH), with $\alpha = 1/3^{1/2} = 0.577$, Eq. (10.25) predicts

$$A = y_{\text{HH}}^2 [2(1 + 0.577^2)^{1/2} - 0.577] = 1.732 y_{\text{HH}}^2 = 3.214$$

or $y_{\text{HH}} = 1.362 \text{ m}$, whence $R_h = \frac{1}{2}y = 0.681 \text{ m}$. The half-hexagon flow rate is thus

$$Q = \frac{1.0}{0.015} (3.214)(0.681)^{2/3} (0.001)^{1/2} = 5.25 \text{ m}^3/\text{s}$$

or about 5 percent more than that for the rectangle.

For a semicircle, $A = 3.214 \text{ m}^2 = \pi D^2/8$, or $D = 2.861 \text{ m}$, whence $P = \frac{1}{2}\pi D = 4.494 \text{ m}$ and $R_h = A/P = 3.214/4.494 = 0.715 \text{ m}$. The semicircle flow rate will thus be

$$Q = \frac{1.0}{0.015} (3.214)(0.715)^{2/3} (0.001)^{1/2} = 5.42 \text{ m}^3/\text{s}$$

or about 8 percent more than that of the rectangle and 3 percent more than that of the half-hexagon.

10.4 Specific Energy; Critical Depth

As suggested by Bakhmeteff [13] in 1911, the specific energy E is a useful parameter in channel flow

$$E = y + \frac{V^2}{2g} \quad (10.28)$$

where y is the water depth. It is seen from Fig. 10.8a that E is the height of the *energy grade line* (EGL) above the channel bottom. For a given flow rate, there are usually two states possible for the same specific energy.

Rectangular Channels

Consider the possible states at a given location. Let $q = Q/b = Vy$ be the discharge per unit width of a rectangular channel. Then, with q constant, Eq. (10.28) becomes

$$E = y + \frac{q^2}{2gy^2} \quad q = \frac{Q}{b} \quad (10.29)$$

Figure 10.8b is a plot of y versus E for constant q from Eq. (10.29). There is a minimum value of E at a certain value of y called the *critical depth*. By setting $dE/dy = 0$ at constant q , we find that E_{\min} occurs at

$$y = y_c = \left(\frac{q^2}{g}\right)^{1/3} = \left(\frac{Q^2}{b^2g}\right)^{1/3} \quad (10.30)$$

The associated minimum energy is

$$E_{\min} = E(y_c) = \frac{3}{2}y_c \quad (10.31)$$

The depth y_c corresponds to channel velocity equal to the shallow-water wave propagation speed C_0 from Eq. (10.10). To see this, rewrite Eq. (10.30) as

$$q^2 = gy_c^3 = (gy_c)y_c^2 = V_c^2y_c^2 \quad (10.32)$$

By comparison it follows that the critical channel velocity is

$$V_c = (gy_c)^{1/2} = C_0 \quad \text{Fr} = 1 \quad (10.33)$$

For $E < E_{\min}$ no solution exists in Fig. 10.8b, and thus such a flow is impossible physically. For $E > E_{\min}$ two solutions are possible: (1) large depth with $V < V_c$, called *subcritical*, and (2) small depth with $V > V_c$, called *supercritical*. In subcritical flow, disturbances can propagate upstream because wave speed $C_0 > V$. In supercritical flow, waves are swept downstream: Upstream is a zone of silence, and a small obstruction in the flow will create a wedge-shaped wave exactly analogous to the Mach waves in

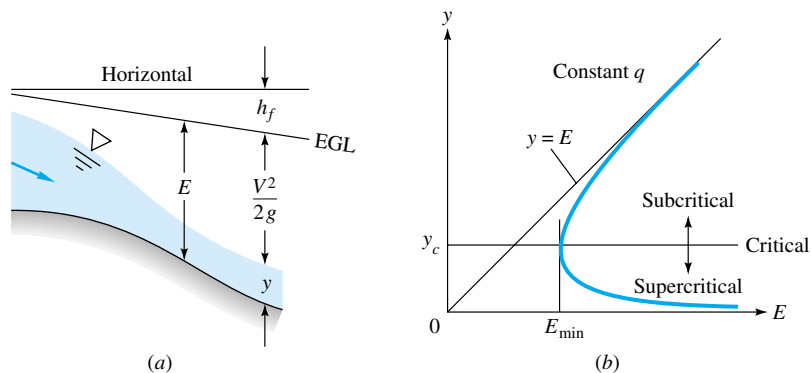


Fig. 10.8 Specific-energy considerations: (a) illustration sketch; (b) depth versus E from Eq. (10.29), showing minimum specific energy occurring at critical depth.

Fig. 9.18c.² The angle of these waves must be

$$\mu = \sin^{-1} \frac{c_0}{V} = \sin^{-1} \frac{(gy)^{1/2}}{V} \quad (10.34)$$

The wave angle and the depth can thus be used as a simple measurement of supercritical-flow velocity.

Note from Fig. 10.8b that small changes in E near E_{\min} cause a large change in the depth y , by analogy with small changes in duct area near the sonic point in Fig. 9.7. Thus critical flow is neutrally stable and is often accompanied by waves and undulations in the free surface. Channel designers should avoid long runs of near-critical flow.

EXAMPLE 10.4

A wide rectangular clean-earth channel has a flow rate $q = 50 \text{ ft}^3/(\text{s} \cdot \text{ft})$. (a) What is the critical depth? (b) What type of flow exists if $y = 3 \text{ ft}$?

Solution

Part (a) From Table 10.1, $n \approx 0.022$ and $\epsilon \approx 0.12 \text{ ft}$. The critical depth follows from Eq. (10.30):

$$y_c = \left(\frac{q^2}{g}\right)^{1/3} = \left(\frac{50^2}{32.2}\right)^{1/3} = 4.27 \text{ ft} \quad \text{Ans. (a)}$$

Part (b) If the actual depth is 3 ft, which is less than y_c , the flow must be *supercritical*. Ans. (b)

Nonrectangular Channels

If the channel width varies with y , the specific energy must be written in the form

$$E = y + \frac{Q^2}{2gA^2} \quad (10.35)$$

The critical point of minimum energy occurs where $dE/dy = 0$ at constant Q . Since $A = A(y)$, Eq. (10.35) yields, for $E = E_{\min}$,

$$\frac{dA}{dy} = \frac{gA^3}{Q^2} \quad (10.36)$$

But $dA = b_0 dy$, where b_0 is the channel width at the free surface. Therefore Eq. (10.36) is equivalent to

$$A_c = \left(\frac{b_0 Q^2}{g}\right)^{1/3} \quad (10.37a)$$

$$V_c = \frac{Q}{A_c} = \left(\frac{gA_c}{b_0}\right)^{1/2} \quad (10.37b)$$

For a given channel shape $A(y)$ and $b_0(y)$ and a given Q , Eq. (10.37) has to be solved by trial and error or by EES to find the critical area A_c , from which V_c can be computed.

²This is the basis of the water-channel analogy for supersonic gas-dynamics experimentation [14, chap. 11].

By comparing the actual depth and velocity with the critical values, we can determine the local flow condition

$$y > y_c, V < V_c: \quad \text{subcritical flow (Fr} < 1)$$

$$y < y_c, V > V_c: \quad \text{supercritical flow (Fr} > 1)$$

Critical Uniform Flow: The Critical Slope

If a critical channel flow is also moving uniformly (at constant depth), it must correspond to a *critical slope* S_c , with $y_n = y_c$. This condition is analyzed by equating Eq. (10.37a) to the Chézy (or Manning) formula:

$$Q^2 = \frac{gA_c^3}{b_0} = C^2 A_c^2 R_h S_c = \frac{\alpha^2}{n^2} A_c^2 R_h^{4/3} S_c$$

$$\text{or} \quad S_c = \frac{n^2 g A_c}{\alpha^2 b_0 R_{hc}^{4/3}} = \frac{n^2 g}{\alpha^2 R_{hc}^{1/3}} \frac{P}{b_0} = \frac{f}{8} \frac{P}{b_0} \quad (10.38)$$

where α^2 equals 1.0 for SI units and 2.208 for BG units. Equation (10.38) is valid for any channel shape. For a wide rectangular channel, $b_0 \gg y_c$, the formula reduces to

$$\text{Wide rectangular channel:} \quad S_c \approx \frac{n^2 g}{\alpha^2 y_c^{1/3}} \approx \frac{f}{8}$$

This is a special case, a reference point. In most channel flows $y_n \neq y_c$. For fully rough turbulent flow, the critical slope varies between 0.002 and 0.008.

EXAMPLE 10.5

Part (a) The 50° triangular channel in Fig. E10.5 has a flow rate $Q = 16 \text{ m}^3/\text{s}$. Compute (a) y_c , (b) V_c , and (c) S_c if $n = 0.018$.

Solution

This is an easy cross section because all geometric quantities can be written directly in terms of depth y

$$\begin{aligned} P &= 2y \csc 50^\circ & A &= y^2 \cot 50^\circ \\ R_h &= \frac{1}{2}y \cos 50^\circ & b_0 &= 2y \cot 50^\circ \end{aligned} \quad (1)$$

The critical-flow condition satisfies Eq. (10.37a)

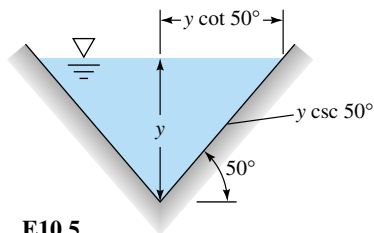
$$gA_c^3 = b_0 Q^2$$

$$\text{or} \quad g(y_c^2 \cot 50^\circ)^3 = (2y_c \cot 50^\circ) Q^2$$

$$y_c = \left(\frac{2Q^2}{g \cot^2 50^\circ} \right)^{1/5} = \left[\frac{2(16)^2}{9.81(0.839)^2} \right]^{1/5} = 2.37 \text{ m} \quad \text{Ans. (a)}$$

Part (b) With y_c known, from Eqs. (1) we compute $P_c = 6.18 \text{ m}$, $R_{hc} = 0.760 \text{ m}$, $A_c = 4.70 \text{ m}^2$, and $b_{0c} = 3.97 \text{ m}$. The critical velocity from Eq. (10.37b) is

$$V_c = \frac{Q}{A} = \frac{16 \text{ m}^3/\text{s}}{4.70 \text{ m}^2} = 3.41 \text{ m/s} \quad \text{Ans. (b)}$$



E10.5

Part (c) With $n = 0.018$, we compute from Eq. (10.38) a critical slope

$$S_c = \frac{gn^2P}{\alpha^2 R_h^{1/3} b_0} = \frac{9.81(0.018)^2(6.18)}{1.0(0.760)^{1/3}(3.97)} = 0.00542 \quad \text{Ans. (c)}$$

Frictionless Flow over a Bump

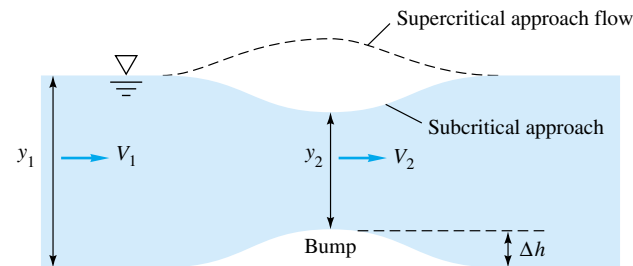
A rough analogy to compressible gas flow in a nozzle (Fig. 9.12) is open-channel flow over a bump, as in Fig. 10.9a. The behavior of the free surface is sharply different according to whether the approach flow is subcritical or supercritical. The height of the bump also can change the character of the results. For frictionless two-dimensional flow, sections 1 and 2 in Fig. 10.9a are related by continuity and momentum:

$$V_1 y_1 = V_2 y_2 \quad \frac{V_1^2}{2g} + y_1 = \frac{V_2^2}{2g} + y_2 + \Delta h$$

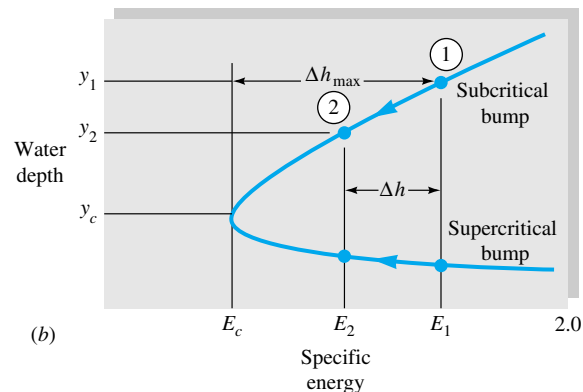
Eliminating V_2 between these two gives a cubic polynomial equation for the water depth y_2 over the bump:

$$y_2^3 - E_2 y_2^2 + \frac{V_1^2 y_1^2}{2g} = 0 \quad \text{where } E_2 = \frac{V_1^2}{2g} + y_1 - \Delta h \quad (10.39)$$

This equation has one negative and two positive solutions if Δh is not too large. Its behavior is illustrated in Fig. 10.9b and depends upon whether condition 1 is on the upper or lower leg of the energy curve. The specific energy E_2 is exactly Δh less than the approach energy E_1 , and point 2 will lie on the same leg of the curve as E_1 . A sub-



(a)



(b)

Fig. 10.9 Frictionless two-dimensional flow over a bump: (a) definition sketch showing Froude-number dependence; (b) specific-energy plot showing bump size and water depths.

critical approach, $Fr_1 < 1$, will cause the water level to decrease at the bump. Supercritical approach flow, $Fr_1 > 1$, causes a water-level increase over the bump.

If the bump height reaches $\Delta h_{\max} = E_1 - E_c$, as illustrated in Fig. 10.9b, the flow at the crest will be exactly critical ($Fr = 1$). If $\Delta h > \Delta h_{\max}$, there are no physically correct solutions to Eq. (10.39). That is, a bump too large will “choke” the channel and cause frictional effects, typically a hydraulic jump (Sec. 10.5).

These bump arguments are reversed if the channel has a *depression* ($\Delta h < 0$): Subcritical approach flow will cause a water-level rise and supercritical flow a fall in depth. Point 2 will be $|\Delta h|$ to the right of point 1, and critical flow cannot occur.

EXAMPLE 10.6

Water flow in a wide channel approaches a 10-cm-high bump at 1.5 m/s and a depth of 1 m. Estimate (a) the water depth y_2 over the bump and (b) the bump height which will cause the crest flow to be critical.

Solution

Part (a) First check the approach Froude number, assuming $C_0 = \sqrt{gy}$:

$$Fr_1 = \frac{V_1}{\sqrt{gy_1}} = \frac{1.5 \text{ m/s}}{\sqrt{(9.81 \text{ m/s}^2)(1.0 \text{ m})}} = 0.479 \quad (\text{subcritical})$$

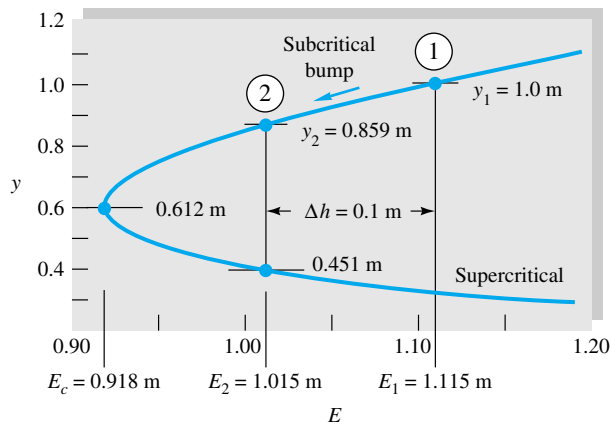
For subcritical approach flow, if Δh is not too large, we expect a depression in the water level over the bump and a higher subcritical Froude number at the crest. With $\Delta h = 0.1$ m, the specific-energy levels must be

$$E_1 = \frac{V_1^2}{2g} + y_1 = \frac{(1.5)^2}{2(9.81)} + 1.0 = 1.115 \quad E_2 = E_1 - \Delta h = 1.015 \text{ m}$$

This physical situation is shown on a specific-energy plot in Fig. E10.6. With y_1 in meters, Eq. (10.39) takes on the numerical values

$$y_2^3 - 1.015y_2^2 + 0.115 = 0$$

There are three real roots: $y_2 = +0.859$ m, $+0.451$ m, and -0.296 m. The third (negative) solution is physically impossible. The second (smaller) solution is the *supercritical* condition for



E10.6

E

E_2 and is not possible for this subcritical bump. The first solution is correct:

$$y_2(\text{subcritical}) \approx 0.859 \text{ m} \quad \text{Ans. (a)}$$

The surface level has dropped by $y_1 - y_2 - \Delta h = 1.0 - 0.859 - 0.1 = 0.041$ m. The crest velocity is $V_2 = V_1 y_1 / y_2 = 1.745$ m/s. The Froude number at the crest is $\text{Fr}_2 = 0.601$. Flow downstream of the bump is subcritical. These flow conditions are shown in Fig. E10.6.

Part (b) For critical flow in a wide channel, with $q = Vy = 1.5 \text{ m}^2/\text{s}$, from Eq. (10.31),

$$E_{2,\min} = E_c = \frac{3}{2} y_c = \frac{3}{2} \left(\frac{q^2}{g} \right)^{1/3} = \frac{3}{2} \left[\frac{(1.5 \text{ m}^2/\text{s})^2}{9.81 \text{ m/s}^2} \right]^{1/3} = 0.918 \text{ m}$$

Therefore the maximum height for frictionless flow over this particular bump is

$$\Delta h_{\max} = E_1 - E_{2,\min} = 1.115 - 0.918 = 0.197 \text{ m} \quad \text{Ans. (b)}$$

For this bump, the solution of Eq. (10.39) is $y_2 = y_c = 0.612$ m, and the Froude number is unity at the crest. At critical flow the surface level has dropped by $y_1 - y_2 - \Delta h = 0.191$ m.

Flow under a Sluice Gate

A sluice gate is a bottom opening in a wall, as sketched in Fig. 10.10a, commonly used in control of rivers and channel flows. If the flow is allowed free discharge through the gap, as in Fig. 10.10a, the flow smoothly accelerates from subcritical (upstream) to critical (near the gap) to supercritical (downstream). The gate is then analogous to a converging-diverging nozzle in gas dynamics, as in Fig. 9.12, operating at its *design condition* (similar to point *H* in Fig. 9.12b).

For free discharge, friction may be neglected, and since there is no bump ($\Delta h = 0$), Eq. (10.39) applies with $E_1 = E_2$:

$$y_2^3 - \left(\frac{V_1^2}{2g} + y_1 \right) y_2^2 + \frac{V_1^2 y_1^2}{2g} = 0 \quad (10.40)$$

Given subcritical upstream flow (V_1, y_1), this cubic equation has only one positive real solution: supercritical flow at the same specific energy, as in Fig. 10.10b. The flow rate varies with the ratio y_2/y_1 ; we ask, as a problem exercise, to show that the flow rate is a maximum when $y_2/y_1 = \frac{2}{3}$.

The free discharge, Fig. 10.10a, contracts to a depth y_2 about 40 percent less than the gate's gap height, as shown. This is similar to a free *orifice* discharge, as in Fig. 6.38. If H is the height of the gate gap and b is the gap width into the paper, we can approximate the flow rate by orifice theory:

$$Q = C_d H b \sqrt{2g y_1} \quad \text{where} \quad C_d \approx \frac{0.61}{\sqrt{1 + 0.61 H / y_1}} \quad (10.41)$$

in the range $H/y_1 < 0.5$. Thus a continuous variation in flow rate is accomplished by raising the gate.

If the tailwater is high, as in Fig. 10.10c, free discharge is not possible. The sluice gate is said to be *drowned* or partially drowned. There will be energy dissipation in the exit flow, probably in the form of a drowned hydraulic jump, and the downstream flow will return to subcritical. Equations (10.40) and (10.41) do not apply to this situation, and experimental discharge correlations are necessary [2, 15]. See Prob. 10.77.

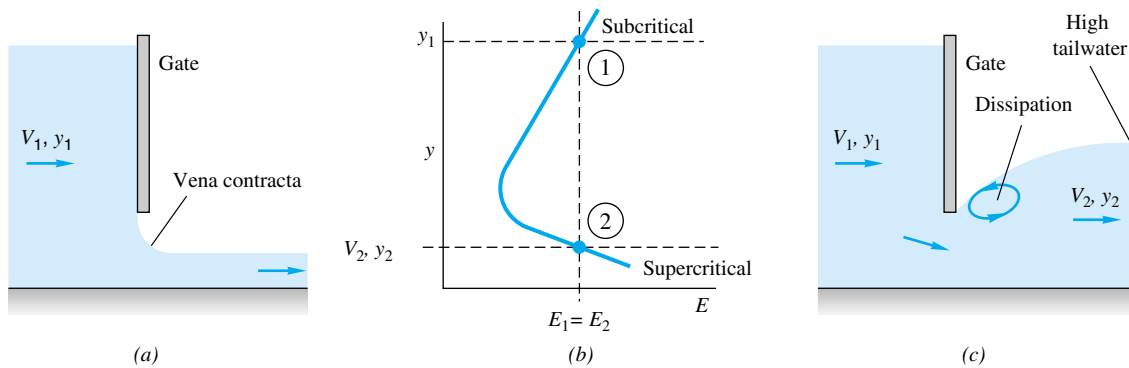


Fig. 10.10 Flow under a sluice gate passes through critical flow: (a) free discharge with vena contracta; (b) specific energy for free discharge; (c) dissipative flow under a drowned gate.

10.5 The Hydraulic Jump

In open-channel flow a supercritical flow can change quickly back to a subcritical flow by passing through a hydraulic jump, as in Fig. 10.5. The upstream flow is fast and shallow, and the downstream flow is slow and deep, analogous to the normal-shock wave of Fig. 9.8. Unlike the infinitesimally thin normal shock, the hydraulic jump is quite thick, ranging in length from 4 to 6 times the downstream depth y_2 [16].

Being extremely turbulent and agitated, the hydraulic jump is a very effective energy dissipator and is a feature of stilling-basin and spillway applications [16]. Figure 10.11 shows the jump formed at the bottom of a dam spillway in a model test. It is very important that such jumps be located on specially designed aprons; otherwise the channel bottom will be badly scoured by the agitation. Jumps also mix fluids very effectively and have application to sewage and water treatment designs.

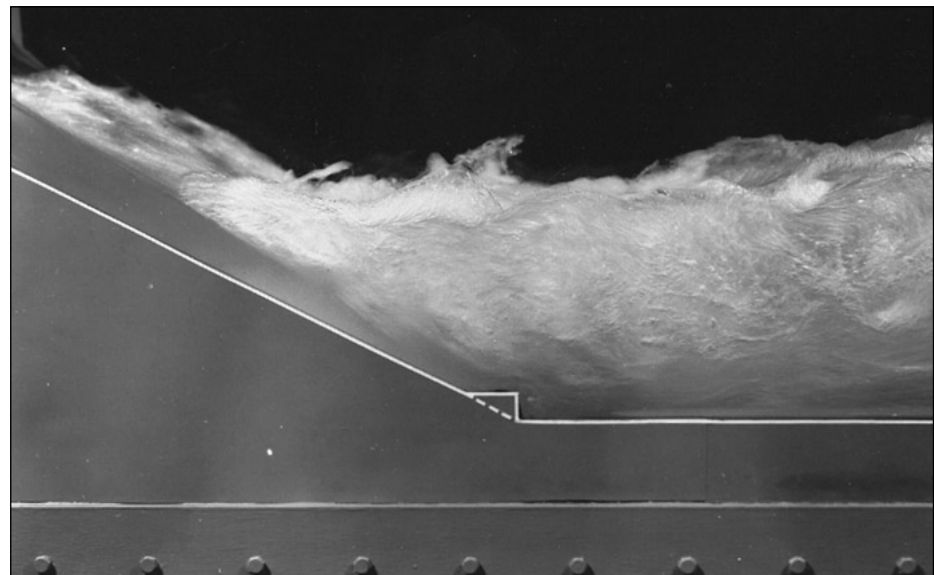


Fig. 10.11 Hydraulic jump formed on a spillway model for the Karnafuli Dam in East Pakistan. (Courtesy of the St. Anthony Falls Hydraulic Laboratory, University of Minnesota.)

Classification

The principal parameter affecting hydraulic-jump performance is the upstream Froude number $Fr_1 = V_1/(gy_1)^{1/2}$. The Reynolds number and channel geometry have only a secondary effect. As detailed in Ref. 16, the following ranges of operation can be outlined, as illustrated in Fig. 10.12:

- $Fr_1 < 1.0$: Jump impossible, violates second law of thermodynamics.
- $Fr_1 = 1.0$ to 1.7: Standing-wave, or *undular jump* about $4y_2$ long; low dissipation, less than 5 percent.
- $Fr_1 = 1.7$ to 2.5: Smooth surface rise with small rollers, known as a *weak jump*; dissipation 5 to 15 percent.

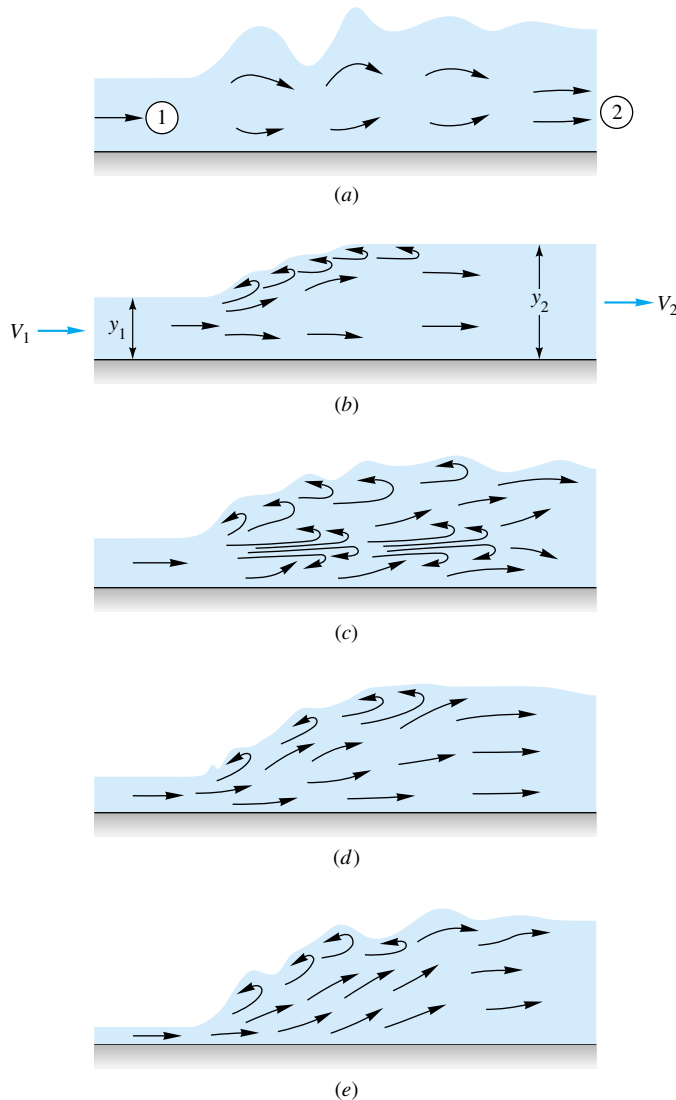


Fig. 10.12 Classification of hydraulic jumps: (a) $Fr = 1.0$ to 1.7: undular jumps; (b) $Fr = 1.7$ to 2.5: weak jump; (c) $Fr = 2.5$ to 4.5: oscillating jump; (d) $Fr = 4.5$ to 9.0: steady jump; (e) $Fr > 9.0$: strong jump. (Adapted from Ref. 16.)

- $Fr_1 = 2.5$ to 4.5 : Unstable, *oscillating jump*; each irregular pulsation creates a large wave which can travel downstream for miles, damaging earth banks and other structures. Not recommended for design conditions. Dissipation 15 to 45 percent.
- $Fr_1 = 4.5$ to 9.0 : Stable, well-balanced, *steady jump*; best performance and action, insensitive to downstream conditions. Best design range. Dissipation 45 to 70 percent.
- $Fr_1 > 9.0$: Rough, somewhat intermittent *strong jump*, but good performance. Dissipation 70 to 85 percent.

Further details can be found in Ref. 16 and Ref. 3, chap. 15.

Theory for a Horizontal Jump

A jump which occurs on a steep channel slope can be affected by the difference in water-weight components along the flow. The effect is small, however, so that the classic theory assumes that the jump occurs on a horizontal bottom.

You will be pleased to know that we have already analyzed this problem in Sec. 10.1. A hydraulic jump is exactly equivalent to the strong fixed wave in Fig. 10.4*b*, where the change in depth δy is not neglected. If V_1 and y_1 upstream are known, V_2 and y_2 are computed by applying continuity and momentum across the wave, as in Eqs. (10.7) and (10.8). Equation (10.9) is therefore the correct solution for a jump if we interpret C and y in Fig. 10.4*b* as upstream conditions V_1 and y_1 , with $C - \delta V$ and $y + \delta y$ being the downstream conditions V_2 and y_2 , as in Fig. 10.12*b*. Equation (10.9) becomes

$$V_1^2 = \frac{1}{2}gy_1\eta(\eta + 1) \quad (10.42)$$

where $\eta = y_2/y_1$. Introducing the Froude number $Fr_1 = V_1/(gy_1)^{1/2}$ and solving this quadratic equation for η , we obtain

$$\frac{2y_2}{y_1} = -1 + (1 + 8 Fr_1^2)^{1/2} \quad (10.43)$$

With y_2 thus known, V_2 follows from the wide-channel continuity relation

$$V_2 = \frac{V_1 y_1}{y_2} \quad (10.44)$$

Finally, we can evaluate the dissipation head loss across the jump from the steady-flow energy equation

$$h_f = E_1 - E_2 = \left(y_1 + \frac{V_1^2}{2g} \right) - \left(y_2 + \frac{V_2^2}{2g} \right)$$

Introducing y_2 and V_2 from Eqs. (10.43) and (10.44), we find after considerable algebraic manipulation that

$$h_f = \frac{(y_2 - y_1)^3}{4y_1 y_2} \quad (10.45)$$

Equation (10.45) shows that the dissipation loss is positive only if $y_2 > y_1$, which is a requirement of the second law of thermodynamics. Equation (10.43) then requires that

$Fr_1 > 1.0$; that is, the upstream flow must be supercritical. Finally, Eq. (10.44) shows that $V_2 < V_1$ and the downstream flow is subcritical. All these results agree with our previous experience analyzing the normal-shock wave.

The present theory is for hydraulic jumps in wide horizontal channels. For the theory of prismatic or sloping channels see advanced texts [for example, 3, chaps. 15 and 16].

EXAMPLE 10.7

Water flows in a wide channel at $q = 10 \text{ m}^3/(\text{s} \cdot \text{m})$ and $y_1 = 1.25 \text{ m}$. If the flow undergoes a hydraulic jump, compute (a) y_2 , (b) V_2 , (c) Fr_2 , (d) h_f , (e) the percentage dissipation, (f) the power dissipated per unit width, and (g) the temperature rise due to dissipation if $c_p = 4200 \text{ J}/(\text{kg} \cdot \text{K})$.

Solution

Part (a) The upstream velocity is

$$V_1 = \frac{q}{y_1} = \frac{10 \text{ m}^3/(\text{s} \cdot \text{m})}{1.25 \text{ m}} = 8.0 \text{ m/s}$$

The upstream Froude number is therefore

$$Fr_1 = \frac{V_1}{(gy_1)^{1/2}} = \frac{8.0}{[9.81(1.25)]^{1/2}} = 2.285$$

From Fig. 10.12 this is a weak jump. The depth y_2 is obtained from Eq. (10.43):

$$\frac{2y_2}{y_1} = -1 + [1 + 8(2.285)^2]^{1/2} = 5.54$$

or

$$y_2 = \frac{1}{2}y_1(5.54) = \frac{1}{2}(1.25)(5.54) = 3.46 \text{ m} \quad \text{Ans. (a)}$$

Part (b) From Eq. (10.44) the downstream velocity is

$$V_2 = \frac{V_1 y_1}{y_2} = \frac{8.0(1.25)}{3.46} = 2.89 \text{ m/s} \quad \text{Ans. (b)}$$

Part (c) The downstream Froude number is

$$Fr_2 = \frac{V_2}{(gy_2)^{1/2}} = \frac{2.89}{[9.81(3.46)]^{1/2}} = 0.496 \quad \text{Ans. (c)}$$

Part (d) As expected, Fr_2 is subcritical. From Eq. (10.45) the dissipation loss is

$$h_f = \frac{(3.46 - 1.25)^3}{4(3.46)(1.25)} = 0.625 \text{ m} \quad \text{Ans. (d)}$$

Part (e) The percentage dissipation relates h_f to upstream energy

$$E_1 = y_1 + \frac{V_1^2}{2g} = 1.25 + \frac{(8.0)^2}{2(9.81)} = 4.51 \text{ m}$$

Hence $\text{Percentage loss} = (100) \frac{h_f}{E_1} = \frac{100(0.625)}{4.51} = 14 \text{ percent} \quad \text{Ans. (e)}$

Part (f) The power dissipated per unit width is

$$\begin{aligned}\text{Power} &= \rho g q h_f = (9800 \text{ N/m}^3)[10 \text{ m}^3/(\text{s} \cdot \text{m})](0.625 \text{ m}) \\ &= 61.3 \text{ kW/m}\end{aligned}\quad \text{Ans. (f)}$$

Part (g) Finally the mass flow rate is $\dot{m} = \rho q = (1000 \text{ kg/m}^3)[10 \text{ m}^3/(\text{s} \cdot \text{m})] = 10,000 \text{ kg}/(\text{s} \cdot \text{m})$, and the temperature rise from the steady-flow energy equation is

$$\text{Power dissipated} = \dot{m} c_p \Delta T$$

$$\text{or} \quad 61,300 \text{ W/m} = [10,000 \text{ kg}/(\text{s} \cdot \text{m})][4200 \text{ J}/(\text{kg} \cdot \text{K})] \Delta T$$

from which

$$\Delta T = 0.0015 \text{ K} \quad \text{Ans. (g)}$$

The dissipation is large, but the temperature rise is negligible.

10.6 Gradually Varied Flow³

In practical channel flows both the bottom slope and the water depth change with position, as in Fig. 10.3. An approximate analysis is possible if the flow is gradually varied, e.g., if the slopes are small and changes not too sudden. The basic assumptions are

1. Slowly changing bottom slope
2. Slowly changing water depth (no hydraulic jumps)
3. Slowly changing cross section
4. One-dimensional velocity distribution
5. Pressure distribution approximately hydrostatic

The flow then satisfies the continuity relation (10.1) plus the energy equation with bottom friction losses included. The two unknowns for steady flow are velocity $V(x)$ and water depth $y(x)$, where x is distance along the channel.

Basic Differential Equation

Consider the length of channel dx illustrated in Fig. 10.13. All the terms which enter the steady-flow energy equation are shown, and the balance between x and $x + dx$ is

$$\frac{V^2}{2g} + y + S_0 dx = S dx + \frac{V^2}{2g} + d \left(\frac{V^2}{2g} \right) + y + dy$$

$$\text{or} \quad \frac{dy}{dx} + \frac{d}{dx} \left(\frac{V^2}{2g} \right) = S_0 - S \quad (10.46)$$

where S_0 is the slope of the channel bottom (positive as shown in Fig. 10.13) and S is the slope of the EGL (which drops due to wall friction losses).

To eliminate the velocity derivative, differentiate the continuity relation

$$\frac{dQ}{dx} = 0 = A \frac{dV}{dx} + V \frac{dA}{dx} \quad (10.47)$$

³This section may be omitted without loss of continuity.

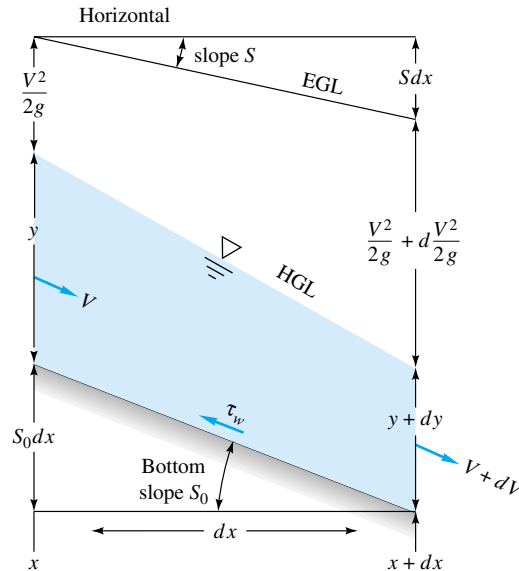


Fig. 10.13 Energy balance between two sections in a gradually varied open-channel flow.

But $dA = b_0 dy$, where b_0 is the channel width at the surface. Eliminating dV/dx between Eqs. (10.46) and (10.47), we obtain

$$\frac{dy}{dx} \left(1 - \frac{V^2 b_0}{gA} \right) = S_0 - S \quad (10.48)$$

Finally, recall from Eq. (10.37) that $V^2 b_0 / (gA)$ is the square of the Froude number of the local channel flow. The final desired form of the gradually varied flow equation is

$$\frac{dy}{dx} = \frac{S_0 - S}{1 - Fr^2} \quad (10.49)$$

This equation changes sign according as the Froude number is subcritical or supercritical and is analogous to the one-dimensional gas-dynamic area-change formula (9.40).

The numerator of Eq. (10.49) changes sign according as S_0 is greater or less than S , which is the slope equivalent to uniform flow at the same discharge Q

$$S = S_{0n} = \frac{f}{D_h} \frac{V^2}{2g} = \frac{V^2}{R_h C^2} = \frac{n^2 V^2}{\alpha^2 R_h^{4/3}} \quad (10.50)$$

where C is the Chézy coefficient. The behavior of Eq. (10.49) thus depends upon the relative magnitude of the local bottom slope $S_0(x)$, compared with (1) uniform flow, $y = y_n$, and (2) critical flow, $y = y_c$. As in Eq. (10.38), the dimensional parameter α^2 equals 1.0 for SI units and 2.208 for BG units.

Classification of Solutions

It is customary to compare the actual channel slope S_0 with the critical slope S_c for the same Q from Eq. (10.38). There are five classes for S_0 , giving rise to twelve distinct types of solution curves, all of which are illustrated in Fig. 10.14:

Slope class	Slope notation	Depth class	Solution curves
$S_0 > S_c$	Steep	$y_c > y_n$	S-1, S-2, S-3
$S_0 = S_c$	Critical	$y_c = y_n$	C-1, C-3
$S_0 < S_c$	Mild	$y_c < y_n$	M-1, M-2, M-3
$S_0 = 0$	Horizontal	$y_n = \infty$	H-2, H-3
$S_0 < 0$	Adverse	$y_n = \text{imaginary}$	A-2, A-3

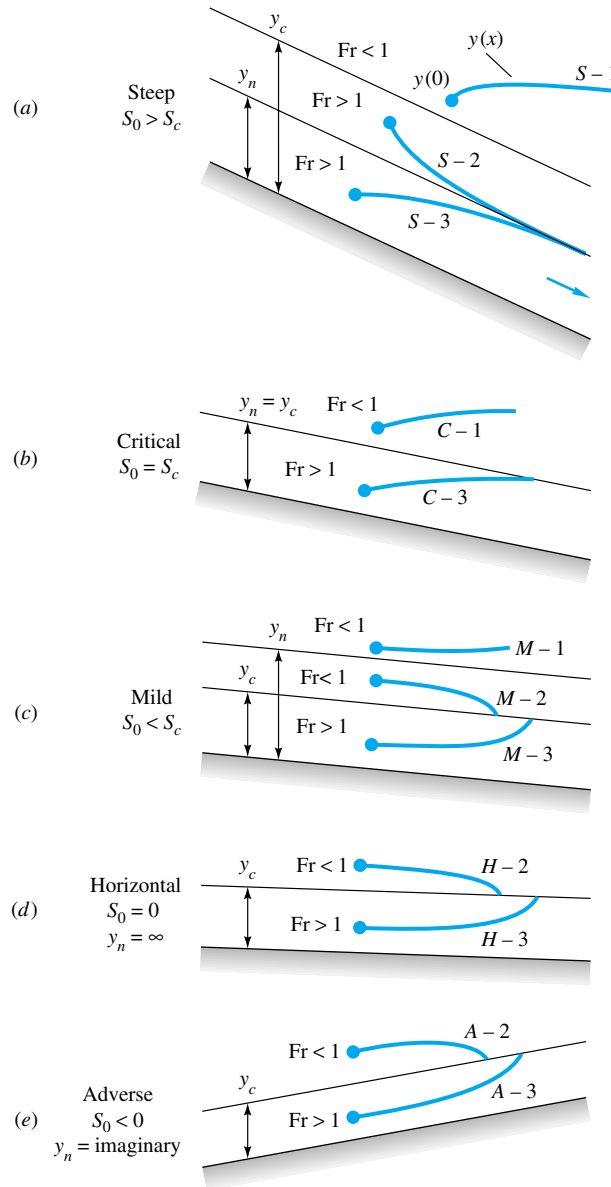


Fig. 10.14 Gradually varied flow for five classes of channel slope, showing the twelve basic solution curves.

The solution letters S, C, M, H, and A obviously denote the names of the five types of slope. The numbers 1, 2, 3 relate to the position of the initial point on the solution curve with respect to the normal depth y_n and the critical depth y_c . In type 1 solutions, the initial point is above both y_n and y_c , and in all cases the water-depth solution $y(x)$ becomes even deeper and farther away from y_n and y_c . In type 2 solutions, the initial point lies between y_n and y_c , and if there is no change in S_0 or roughness, the solution tends asymptotically toward the lower of y_n or y_c . In type 3 cases, the initial point lies below both y_n and y_c , and the solution curve tends asymptotically toward the lower of these.

Figure 10.14 shows the basic character of the local solutions, but in practice, of course, S_0 varies with x and the overall solution patches together the various cases to form a continuous depth profile $y(x)$ compatible with a given initial condition and a given discharge Q . There is a fine discussion of various composite solutions in Ref. 3, chap. 9; see also Ref. 18, sec. 12.7.

Numerical Solution

The basic relation for gradually varied flow, Eq. (10.49), is a first-order ordinary differential equation which can be easily solved numerically. For a given constant-volume flow rate Q , it may be written in the form

$$\frac{dy}{dx} = \frac{S_0 - n^2 Q^2 / (\alpha^2 A^2 R_h^{4/3})}{1 - Q^2 b_0 / (g A^3)} \quad (10.51)$$

subject to an initial condition $y = y_0$ at $x = x_0$. It is assumed that the bottom slope $S_0(x)$ and the cross-sectional shape parameters (b_0 , P , A) are known everywhere along the channel. Then one may solve Eq. (10.51) for local water depth $y(x)$ by any standard numerical method. The author uses an Excel spreadsheet for a personal computer. Step sizes Δx may be selected so that each change Δy is limited to no greater than, say, 1 percent. The solution curves are generally well behaved unless there are discontinuous changes in channel parameters. Note that if one approaches the critical depth y_c , the denominator of Eq. (10.51) approaches zero, so small step sizes are required. It helps physically to know what type solution curve (M-1, S-2, etc.) you are proceeding along, but this is not mathematically necessary.

EXAMPLE 10.8

Let us extend the data of Example 10.4 to compute a portion of the profile shape. Given is a wide channel with $n = 0.022$, $S_0 = 0.0048$, and $q = 50 \text{ ft}^3/(\text{s} \cdot \text{ft})$. If $y_0 = 3 \text{ ft}$ at $x = 0$, how far along the channel $x = L$ does it take the depth to rise to $y_L = 4 \text{ ft}$? Is the 4-ft depth position upstream or downstream in Fig. E10.8a?

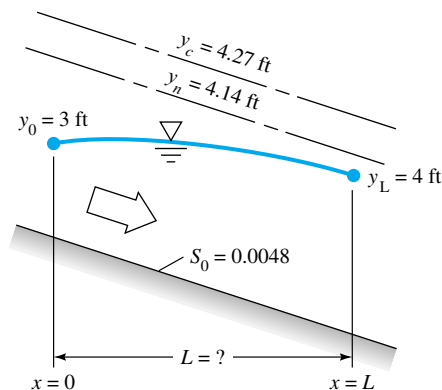
Solution

In Example 10.4 we computed $y_c = 4.27 \text{ ft}$. Since our initial depth $y = 3 \text{ ft}$ is less than y_c , we know the flow is supercritical. Let us also compute the normal depth for the given slope S_0 by setting $q = 50 \text{ ft}^3/(\text{s} \cdot \text{ft})$ in the Chézy formula (10.19) with $R_h = y_n$:

$$q = \frac{\alpha}{n} AR_h^{2/3} S_0^{1/2} = \frac{1.486}{0.022} [y_n(1 \text{ ft})] y_n^{2/3} (0.0048)^{1/2} = 50 \text{ ft}^3/(\text{s} \cdot \text{ft})$$

Solve for:

$$y_n \approx 4.14 \text{ ft}$$



E10.8a

Thus both $y(0) = 3$ ft and $y(L) = 4$ ft are less than y_n , which is less than y_c , so we *must* be on an S-3 curve, as in Fig. 10.14a. For a wide channel, Eq. (10.51) reduces to

$$\frac{dy}{dx} = \frac{S_0 - n^2 q^2 / (\alpha^2 y^{10/3})}{1 - q^2 / (g y^3)}$$

$$\approx \frac{0.0048 - (0.022)^2 (50)^2 / (2.208 y^{10/3})}{1 - (50)^2 / (32.2 y^3)} \quad \text{with } y(0) = 3 \text{ ft}$$

The initial slope is $y'(0) \approx 0.00494$, and a step size $\Delta x = 5$ ft would cause a change $\Delta y \approx (0.00494)(5 \text{ ft}) \approx 0.025$ ft, less than 1 percent. We therefore integrate numerically with $\Delta x = 5$ ft to determine when the depth $y = 4$ ft is achieved. Tabulate some values:

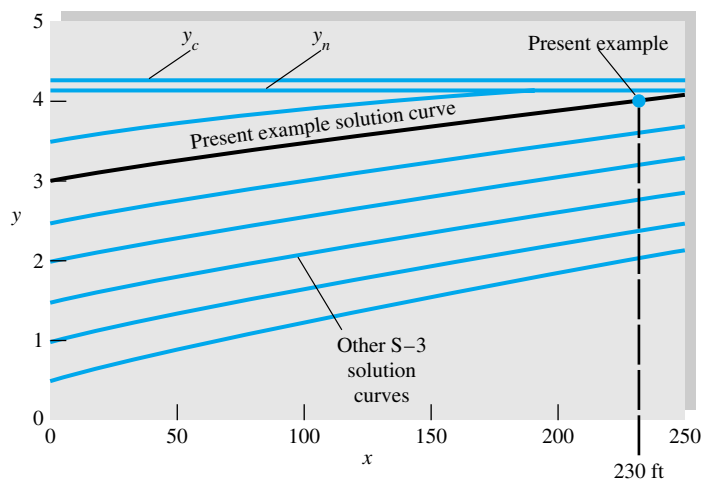
x , ft	0	50	100	150	200	230
y , ft	3.00	3.25	3.48	3.70	3.90	4.00

The water depth, still supercritical, reaches $y = 4$ ft at

$$x \approx 230 \text{ ft downstream}$$

Ans.

We verify from Fig. 10.14a that water depth does increase downstream on an S-3 curve. The solution curve $y(x)$ is shown as the bold line in Fig. E10.8b.



E10.8b

For little extra effort we can investigate the entire family of S-3 solution curves for this problem. Figure E10.8*b* also shows what happens if the initial depth is varied from 0.5 to 3.5 ft in increments of 0.5 ft. All S-3 solutions smoothly rise and asymptotically approach the uniform-flow condition $y = y_n = 4.14$ ft.

Some Illustrative Composite-Flow Profiles

The solution curves in Fig. 10.14 are somewhat simplistic, since they postulate constant bottom slopes. In practice, channel slopes can vary greatly, $S_0 = S_0(x)$, and the solution curves can cross between two regimes. Other parameter changes, such as $A(x)$, $b_0(x)$, and $n(x)$, can cause interesting composite-flow profiles. Some examples are shown in Fig. 10.15.

Figure 10.15*a* shows a change from a mild slope to a steep slope in a constant-width channel. The initial M-2 curve must change to an S-2 curve farther down the steep slope. The only way this can happen physically is for the solution curve to pass smoothly through the critical depth, as shown. The critical point is mathematically *singular* [3, sec. 9.6], and the flow near this point is generally *rapidly*, not gradually, varied. The flow pattern, accelerating from subcritical to supercritical, is similar to a converging-diverging nozzle in gas dynamics. Other scenarios for Fig. 10.15*a* are impossible. For example, the upstream curve cannot be M-1, for the break in slope would cause an S-1 curve which would move away from uniform steep flow.

Figure 10.15*b* shows a mild slope which becomes even milder. The water depth moves smoothly along an M-1 curve to the new (higher) uniform flow. There is no singular point, so gradually varied theory is adequate.

Figure 10.15*c* illustrates a steep slope which becomes less steep. The depth will change smoothly along an S-3 curve to approach the new (higher) uniform flow. There is no singular point. Compare with Fig. 10.15*b*.

Figure 10.15*d* shows a steep slope which changes to mild. It is generally impossible to revert back smoothly from supercritical to subcritical flow without dissipation. A hydraulic jump will form whose position depends upon downstream conditions. Two cases are illustrated: (1) a jump to an S-1 curve to reach a high downstream normal depth and (2) a change to an M-3 curve and then a jump to a lower downstream depth.

Figure 10.15*e* illustrates a *free overfall* with a mild slope. This acts as a *control section* to the upstream flow, which then forms an M-2 curve and accelerates to critical flow near the overfall. The falling stream will be supercritical. The overfall “controls” the water depths upstream and can serve as an initial condition for computation of $y(x)$. This is the type of flow which occurs in a weir or waterfall, Sec. 10.7.

The examples in Fig. 10.15 show that changing conditions in open-channel flow can result in complex flow patterns. Many more examples of composite-flow profiles are given in Refs. 1, 3, and 18.

10.7 Flow Measurement and Control by Weirs

A *weir*, of which the ordinary dam is an example, is a channel obstruction over which the flow must deflect. For simple geometries the channel discharge Q correlates with gravity and with the blockage height H to which the upstream flow is backed up above the weir elevation (see Fig. 10.16). Thus a weir is a simple but effective open-channel flowmeter. We used a weir as an example of dimensional analysis in Prob. 5.32.

Figure 10.16 shows two common weirs, sharp-crested and broad-crested, assumed to be very wide. In both cases the flow upstream is subcritical, accelerates to critical near the top of the weir, and spills over into a supercritical *nappe*. For both weirs the

discharge q per unit width is proportional to $g^{1/2}H^{3/2}$ but with somewhat different coefficients. The short-crested (or thin-plate) weir nappe should be *ventilated* to the atmosphere; i.e., it should spring clear of the weir crest. Unventilated or drowned nappes are more difficult to correlate and depend upon tailwater conditions. (The spillway of Fig. 10.11 is a sort of unventilated weir.)

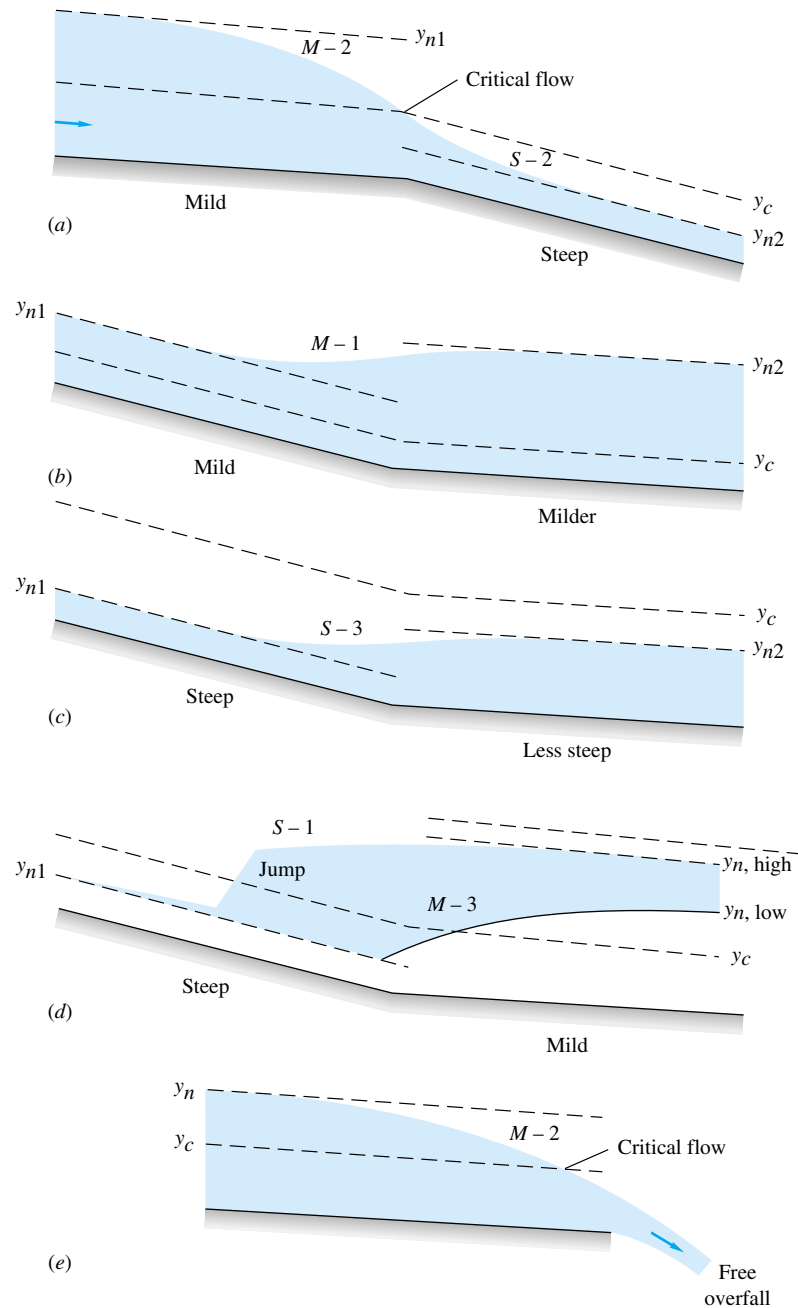


Fig. 10.15 Some examples of composite-flow profiles.

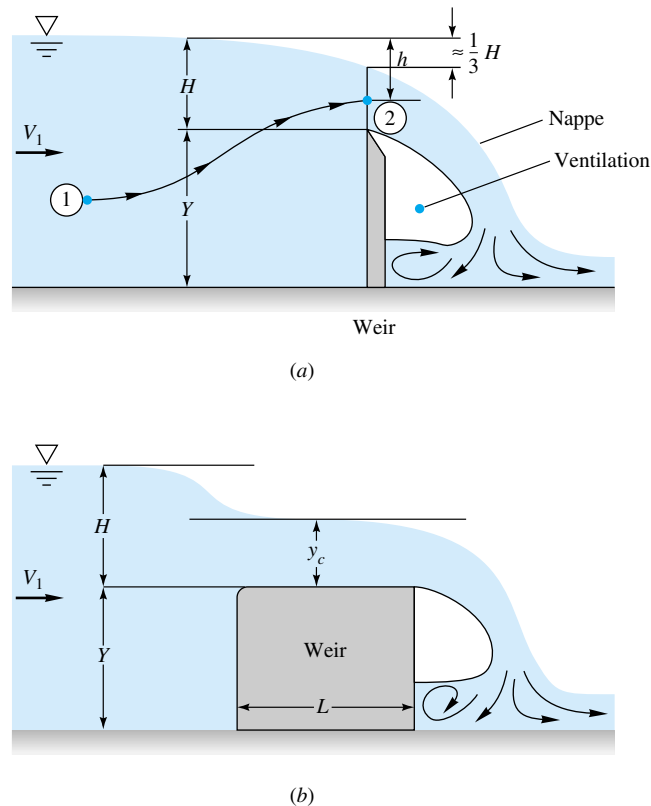


Fig. 10.16 Flow over wide, well-ventilated weirs: (a) sharp-crested; (b) broad-crested.

A very complete discussion of weirs, including other designs such as the polygonal “Crump” weir and various contracting flumes, is given in the text by Ackers et al. [19]. See Prob. 10.122.

Analysis of Sharp-Crested Weirs

It is possible to analyze weir flow by inviscid potential theory with an unknown (but solvable) free surface, as in Fig. P8.71. Here, however, we simply use one-dimensional-flow theory plus dimensional analysis to develop suitable weir flow-rate correlations.

A very early theoretical approach is credited to J. Weisbach in 1855. The velocity head at any point 2 above the weir crest is assumed to equal the total head upstream; i.e., Bernoulli’s equation is used with no losses:

$$\frac{V_2^2}{2g} + H - h \approx \frac{V_1^2}{2g} + H \quad \text{or} \quad V_2(h) \approx \sqrt{2gh + V_1^2}$$

where h is the vertical distance down to point 2, as shown in Fig. 10.16a. If we accept for the moment, without proof, that the flow over the crest draws down to $h_{\min} \approx H/3$, the volume flow $q = Q/b$ over the crest is approximately

$$\begin{aligned} q &= \int_{\text{crest}} V_2 \, dh \approx \int_{H/3}^H (2gh + V_1^2)^{1/2} \, dh \\ &= \frac{2}{3} \sqrt{2g} \left[\left(H + \frac{V_1^2}{2g} \right)^{3/2} - \left(\frac{H}{3} + \frac{V_1^2}{2g} \right)^{3/2} \right] \end{aligned} \quad (10.52)$$

Normally the upstream velocity head $V_1^2/(2g)$ is neglected, so this expression reduces to

$$\text{Sharp-crested theory: } q \approx 0.81\left(\frac{2}{3}\right)(2g)^{1/2}H^{3/2} \quad (10.53)$$

This formula is functionally correct, but the coefficient 0.81 is too high and should be replaced by an experimentally determined discharge coefficient.

Analysis of Broad-Crested Weirs

The broad-crested weir of Fig. 10.16*b* can be analyzed more accurately because it creates a short run of nearly one-dimensional critical flow, as shown. Bernoulli's equation from upstream to the weir crest yields

$$\frac{V_1^2}{2g} + Y + H \approx \frac{V_c^2}{2g} + Y + y_c$$

If the crest is very wide into the paper, $V_c^2 = gy_c$ from Eq. (10.33). Thus we can solve for

$$y_c \approx \frac{2H}{3} + \frac{V_1^2}{3g} \approx \frac{2H}{3}$$

This result was used without proof to derive Eq. (10.53). Finally, the flow rate follows from wide-channel critical flow, Eq. (10.32):

$$\text{Broad-crested theory: } q = \sqrt{gy_c^3} \approx \frac{1}{\sqrt{3}} \left(\frac{2}{3}\right) \sqrt{2g} \left(H + \frac{V_1^2}{2g}\right)^{3/2} \quad (10.54)$$

Again we may usually neglect the upstream velocity head $V_1^2/(2g)$. The coefficient $1/\sqrt{3} \approx 0.577$ is about right, but experimental data are preferred.

Experimental Weir Discharge Coefficients

Theoretical weir-flow formulas may be modified experimentally as follows. Eliminate the numerical coefficients $\frac{2}{3}$ and $\sqrt{2}$, for which there is much sentimental attachment in the literature, and reduce the formula to

$$Q_{\text{weir}} = C_d b \sqrt{g} \left(H + \frac{V_1^2}{2g}\right)^{3/2} \approx C_d b \sqrt{g} H^{3/2} \quad (10.55)$$

where b is the crest width and C_d is a dimensionless, experimentally determined *weir discharge coefficient* which may vary with the weir geometry, Reynolds number, and Weber number. Many data for many different weirs have been reported in the literature, as detailed in Ref. 19.

An accurate (± 2 percent) composite correlation for wide ventilated sharp crests is recommended as follows [19]:

$$\text{Wide sharp-crested weir: } C_d \approx 0.564 + 0.0846 \frac{H}{Y} \quad \text{for} \quad \frac{H}{Y} \leq 2 \quad (10.56)$$

The Reynolds numbers $V_1 H / \nu$ for these data varied from 1 E4 to 2 E6, but the formula should apply to higher Re, such as large dams on rivers.

The broad-crested weir of Fig. 10.16*b* is considerably more sensitive to geometric parameters, including the surface roughness ϵ of the crest. If the leading-edge nose is rounded, $R/L \geq 0.05$, available data [19, chap. 7] may be correlated as follows:

$$\text{Round-nosed broad-crested weir: } C_d \approx 0.544 \left(1 - \frac{\delta^*/L}{H/L}\right)^{3/2} \quad (10.57)$$

where
$$\frac{\delta^*}{L} \approx 0.001 + 0.2\sqrt{\epsilon/L}$$

The chief effect is due to turbulent boundary-layer displacement-thickness growth δ^* on the crest as compared to upstream head H . The formula is limited to $H/L < 0.7$, $\epsilon/L \leq 0.002$, and $V_1 H/\nu > 3 \text{ E}5$. If the nose is round, there is no significant effect of weir height Y , at least if $H/Y < 2.4$.

If the broad-crested weir has a sharp leading edge, thus commonly called a *rectangular* weir, the discharge may depend upon the weir height Y . However, in a certain range of weir height and length, C_d is nearly constant:

Sharp-nosed
broad-crested weir:
$$C_d \approx 0.462 \quad \text{for} \quad 0.08 < \frac{H}{L} < 0.33$$

$$0.22 < \frac{H}{Y} < 0.56$$
(10.58)

Surface roughness is not a significant factor here. For $H/L < 0.08$ there is large scatter (± 10 percent) in the data. For $H/L > 0.33$ and $H/Y > 0.56$, C_d increases up to 10 percent due to each parameter, and complex charts are needed for the discharge coefficient [19, chap. 6].

EXAMPLE 10.9

A weir in a horizontal channel is 1 m high and 4 m wide. The water depth upstream is 1.6 m. Estimate the discharge if the weir is (a) sharp-crested and (b) round-nosed with an unfinished cement broad crest 1.2 m long. Neglect $V_1^2/(2g)$.

Solution

Part (a) We are given $Y = 1 \text{ m}$ and $H + Y \approx 1.6 \text{ m}$, hence $H \approx 0.6 \text{ m}$. Since $H \ll b$, we assume that the weir is “wide.” For a sharp crest, Eq. (10.56) applies:

$$C_d \approx 0.564 + 0.0846 \frac{0.6 \text{ m}}{1 \text{ m}} \approx 0.615$$

Then the discharge is given by the basic correlation, Eq. (10.55):

$$Q = C_d b \sqrt{g} H^{3/2} = (0.615)(4 \text{ m}) \sqrt{(9.81 \text{ m/s}^2)(0.6 \text{ m})^{3/2}} \approx 3.58 \text{ m}^3/\text{s} \quad \text{Ans. (a)}$$

We check that $H/Y = 0.6 < 2.0$ for Eq. (10.56) to be valid. From continuity, $V_1 = Q/(by_1) = 3.58/[(4.0)(1.6)] = 0.56 \text{ m/s}$, giving a Reynolds number $V_1 H/\nu \approx 3.4 \text{ E}5$.

Part (b) For a round-nosed broad-crested weir, Eq. (10.57) applies. For an unfinished cement surface, read $\epsilon \approx 2.4 \text{ mm}$ from Table 10.1. Then the displacement thickness is

$$\frac{\delta^*}{L} \approx 0.001 + 0.2\sqrt{\epsilon/L} = 0.001 + 0.2\left(\frac{0.0024 \text{ m}}{1.2 \text{ m}}\right)^{1/2} \approx 0.00994$$

Then Eq. (10.57) predicts the discharge coefficient:

$$C_d \approx 0.544 \left(1 - \frac{0.00994}{0.6 \text{ m}/1.2 \text{ m}}\right)^{3/2} \approx 0.528$$

The estimated flow rate is thus

$$Q = C_d b \sqrt{g} H^{3/2} = 0.528(4 \text{ m}) \sqrt{(9.81 \text{ m}^2/\text{s}^2)(0.6 \text{ m})^{3/2}} \approx 3.07 \text{ m}^3/\text{s} \quad \text{Ans. (b)}$$

Check that $H/L = 0.5 < 0.7$ as required. The approach Reynolds number is $V_1 H/\nu \approx 2.9 \text{ E}5$, just barely below the recommended limit in Eq. (10.57).

Since $V_1 \approx 0.5 \text{ m/s}$, $V_1^2/(2g) \approx 0.012 \text{ m}$, so the error in taking total head equal to 0.6 m is about 2 percent. We could correct this for upstream velocity head if desired.

Other Thin-Plate Weir Designs

Weirs are often used for flow measurement and control of artificial channels. The two most common shapes are a rectangle and a V notch, as shown in Table 10.2. All should be fully ventilated and not drowned.

Table 10.2a shows a full-width rectangle, which will have slight end-boundary-layer effects but no end contractions. For a thin-plate design, the top is approximately sharp-crested, and Eq. (10.56) should give adequate accuracy, as shown in the table. Since the overfall spans the entire channel, artificial ventilation may be needed, such as holes in the channel walls.

Table 10.2 Thin-Plate Weirs for Flow Measurement

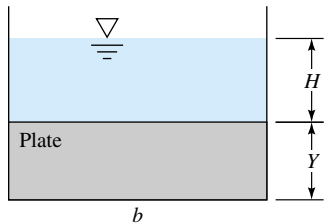
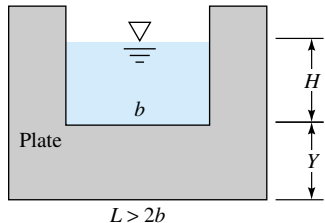
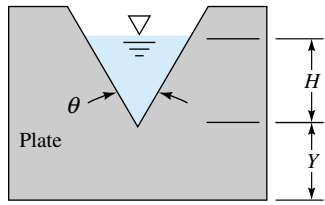
Thin-plate weir	Flow-rate correlation
 <p>(a) Full-width rectangle.</p>	$Q \approx \left(0.564 + 0.0846 \frac{H}{Y} \right) b g^{1/2} H^{3/2}$
 <p>(b) Rectangle with side contractions.</p>	$Q \approx 0.581(b - 0.1H) g^{1/2} H^{3/2} \quad H < 0.5Y$
 <p>(c) V notch.</p>	$Q \approx 0.44 \tan \frac{\theta}{2} g^{1/2} H^{5/2} \quad 20^\circ < \theta < 100^\circ$

Table 10.2*b* shows a partial-width rectangle, $b < L$, which will cause the sides of the overfall to contract inward and reduce the flow rate. An adequate contraction correction [19, 20] is to reduce the effective weir width by $0.1H$, as shown in the table. It seems, however, that this type of weir is rather sensitive to small effects, such as plate thickness and sidewall boundary-layer growth. Small heads ($H < 75$ mm) and small slot widths ($b < 30$ cm) are not recommended. See Refs. 19 and 20 for further details.

The V notch, in Table 10.2*c*, is intrinsically interesting in that its overfall has only one length scale, H —there is no separate “width.” The discharge will thus be proportional to $H^{5/2}$, rather than a power of $\frac{3}{2}$. Application of Bernoulli’s equation to the triangular opening, in the spirit of Eq. (10.52), leads to the following ideal flow rate for a V notch:

$$\text{V notch:} \quad Q_{\text{ideal}} = \frac{8\sqrt{2}}{15} \tan \frac{\theta}{2} g^{1/2} H^{5/2} \quad (10.59)$$

where θ is the total included angle of the notch. The actual measured flow is about 40 percent less than this, due to contraction similar to a thin-plate orifice. In terms of an experimental discharge coefficient, the recommended formula is

$$Q_{\text{V notch}} \approx C_d \tan \frac{\theta}{2} g^{1/2} H^{5/2} \quad C_d \approx 0.44 \quad \text{for} \quad 20^\circ < \theta < 100^\circ \quad (10.60)$$

for heads $H > 50$ mm. For smaller heads, both Reynolds-number and Weber-number effects may be important, and a recommended correction [19] is

$$\text{Low heads, } H < 50 \text{ mm:} \quad C_{d, \text{V notch}} \approx 0.44 + \frac{0.9}{(\text{Re We})^{1/6}} \quad (10.61)$$

where $\text{Re} = \rho g^{1/2} H^{3/2} / \mu$ and $\text{We} = \rho g H^2 / Y$, with Y being the coefficient of surface tension. Liquids other than water may be used with this formula, as long as $\text{Re} > 300 / \tan(\theta/2)^{3/4}$ and $\text{We} > 300$.

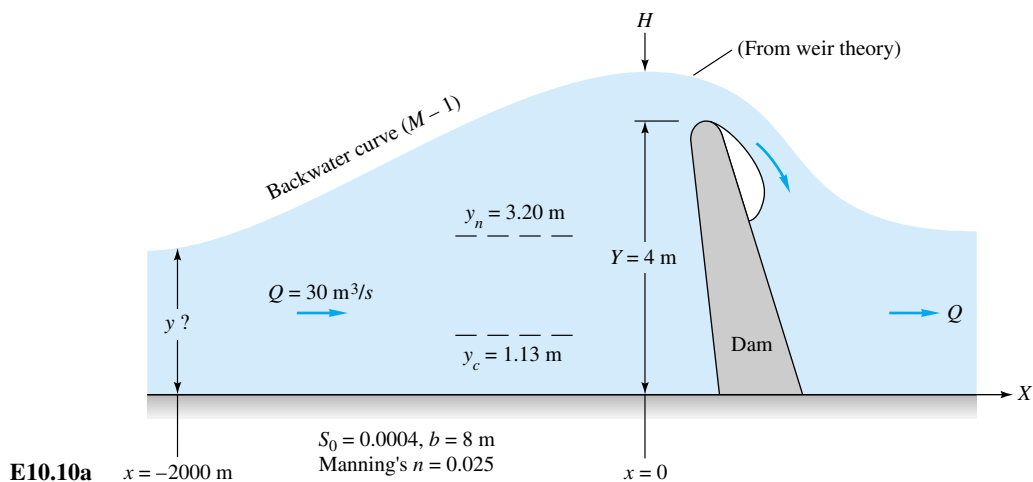
A number of other thin-plate weir designs—trapezoidal, parabolic, circular arc, and U-shaped—are discussed in Ref. 21, which also contains considerable data on broad-crested weirs.

Backwater Curves

A weir is a flow barrier which not only alters the local flow over the weir but also modifies the flow-depth distribution far upstream. Any strong barrier in an open-channel flow creates a *backwater curve*, which can be computed by the gradually varied flow theory of Sec. 10.6. If Q is known, the weir formula, Eq. (10.55), determines H and hence the water depth just upstream of the weir, $y = H + Y$, where Y is the weir height. We then compute $y(x)$ upstream of the weir from Eq. (10.51), following in this case an M-1 curve (Fig. 10.14*c*). Such a barrier, where the water depth correlates with the flow rate, is called a channel *control point*. These are the starting points for numerical analysis of floodwater profiles in rivers as studied, e.g., by the U.S. Army Corps of Engineers [22].

EXAMPLE 10.10

A rectangular channel 8 m wide, with a flow rate of $30 \text{ m}^3/\text{s}$, encounters a 4-m-high sharp-edged dam, as shown in Fig. E10.10*a*. Determine the water depth 2 km upstream if the channel slope is $S_0 = 0.0004$ and $n = 0.025$.



Solution

First determine the head H produced by the dam, using sharp-crested full-width weir theory, Eq. (10.56):

$$Q = 30 \text{ m}^3/\text{s} = C_d b g^{1/2} H^{3/2} = \left(0.564 + 0.0846 \frac{H}{4 \text{ m}} \right) (8 \text{ m}) (9.81 \text{ m/s}^2)^{1/2} H^{3/2}$$

Since the term $0.0846H/4$ in parentheses is small, we may proceed by iteration or EES to the solution $H \approx 1.59$ m. Then our initial condition at $x = 0$, just upstream of the dam, is $y(0) = Y + H = 4 + 1.59 = 5.59$ m. Compare this to the critical depth from Eq. (10.30):

$$y_c = \left(\frac{Q^2}{b^2 g} \right)^{1/3} = \left[\frac{(30 \text{ m}^3/\text{s})^2}{(8 \text{ m})^2 (9.81 \text{ m/s}^2)} \right]^{1/3} = 1.13 \text{ m}$$

Since $y(0)$ is greater than y_c , the flow upstream is subcritical. Finally, for reference purposes, estimate the normal depth from the Chézy equation (10.19):

$$Q = 30 \text{ m}^3/\text{s} = \frac{\alpha}{n} b y R_h^{2/3} S_0^{1/2} = \frac{1.0}{0.025} (8 \text{ m}) y_n \left(\frac{8 y_n}{8 + 2 y_n} \right)^{2/3} (0.0004)^{1/2}$$

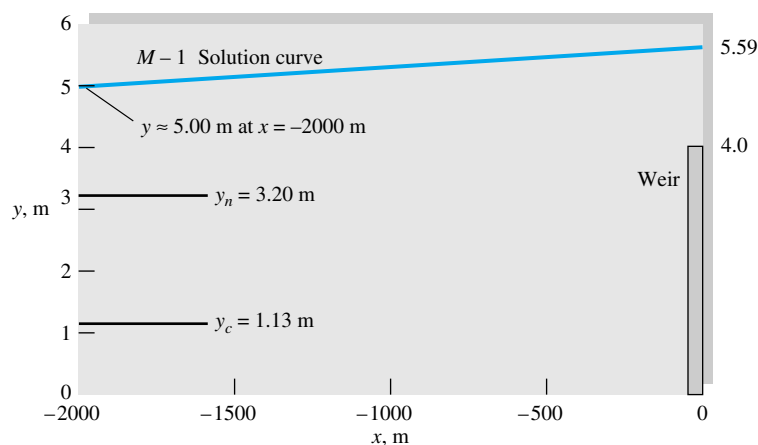
By trial and error or EES solve for $y_n \approx 3.20$ m. If there are no changes in channel width or slope, the water depth far upstream of the dam will approach this value. All these reference values $y(0)$, y_c , and y_n are shown in Fig. E10.10b.

Since $y(0) > y_n > y_c$, the solution will be an M-1 curve as computed from gradually varied theory, Eq. (10.51), for a rectangular channel with the given input data:

$$\frac{dy}{dx} \approx \frac{S_0 - n^2 Q^2 / (\alpha^2 A^2 R_h^{4/3})}{1 - Q^2 b_0 / (g A^3)} \quad \alpha = 1.0 \quad A = 8y \quad n = 0.025 \quad R_h = \frac{8y}{8 + 2y} \quad b_0 = 8$$

Beginning with $y = 5.59$ m at $x = 0$, we integrate backward to $x = -2000$ m. For the Runge-Kutta method, four-figure accuracy is achieved for $\Delta x = -100$ m. The complete solution curve is shown in Fig. E10.10b. The desired solution value is

At $x = -2000$ m: $y \approx 5.00$ m Ans.



E10.10b

Thus, even 2 km upstream, the dam has produced a “backwater” which is 1.8 m above the normal depth which would occur without a dam. For this example, a near-normal depth of, say, 10 cm greater than y_n , or $y \approx 3.3$ m, would not be achieved until $x = -13,400$ m. Backwater curves are quite far-reaching upstream, especially in flood stages.

Summary

This chapter is an introduction to open-channel flow analysis, limited to steady, one-dimensional-flow conditions. The basic analysis combines the continuity equation with the extended Bernoulli equation including friction losses.

Open-channel flows are classified either by depth variation or by Froude number, the latter being analogous to the Mach number in compressible duct flow (Chap. 9). Flow at constant slope and depth is called uniform flow and satisfies the classical Chézy equation (10.19). Straight prismatic channels can be optimized to find the cross section which gives maximum flow rate with minimum friction losses. As the slope and flow velocity increase, the channel reaches a *critical* condition of Froude number unity, where velocity equals the speed of a small-amplitude surface wave in the channel. Every channel has a critical slope which varies with the flow rate and roughness. If the flow becomes supercritical ($Fr > 1$), it may undergo a hydraulic jump to a greater depth and lower (subcritical) velocity, analogous to a normal-shock wave.

The analysis of gradually varied flow leads to a differential equation (10.51) which can be solved by numerical methods. The chapter ends with a discussion of the flow over a dam or weir, where the total flow rate can be correlated with upstream water depth.

Problems

Most of the problems herein are fairly straightforward. More difficult or open-ended assignments are labeled with an asterisk. Problems labeled with an EES icon will benefit from the use of the Engineering Equations Solver (EES), while problems labeled with a computer icon may require the use of a computer. The standard

end-of-chapter problems 10.1 to 10.128 (categorized in the problem list below) are followed by word problems W10.1 to W10.13, fundamentals of engineering exam problems FE10.1 to FE10.7, comprehensive problems C10.1 to C10.3, and design projects D10.1 and D10.2.

Problem distribution

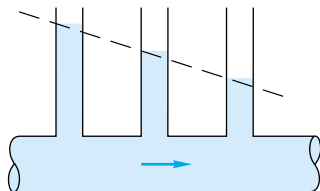
Section	Topic	Problems
10.1	Introduction: Froude number, wave speed	10.1–10.10
10.2	Uniform flow: The Chézy formula	10.11–10.36
10.3	Efficient uniform-flow channels	10.37–10.46
10.4	Specific energy: Critical depth	10.47–10.58
10.4	Flow over a bump	10.59–10.68
10.4	Sluice-gate flow	10.69–10.78
10.5	The hydraulic jump	10.79–10.96
10.6	Gradually varied flow	10.97–10.112
10.7	Weirs and flumes	10.113–10.123
10.7	Backwater curves	10.124–10.128

P10.1 The formula for shallow-water wave propagation speed, Eq. (10.9) or (10.10), is independent of the physical properties of the liquid, i.e., density, viscosity, or surface tension. Does this mean that waves propagate at the same speed in water, mercury, gasoline, and glycerin? Explain.

P10.2 A shallow-water wave 1 cm high propagates into still water of depth 1.1 m. Compute (a) the wave speed c and (b) the induced velocity δV .

P10.3 Narragansett Bay is approximately 21 (statute) mi long and has an average depth of 42 ft. Tidal charts for the area indicate a time delay of 30 min between high tide at the mouth of the bay (Newport, Rhode Island) and its head (Providence, Rhode Island). Is this delay correlated with the propagation of a shallow-water tidal-crest wave through the bay? Explain.

P10.4 The water-channel flow in Fig. P10.4 has a free surface in three places. Does it qualify as an open-channel flow? Explain. What does the dashed line represent?

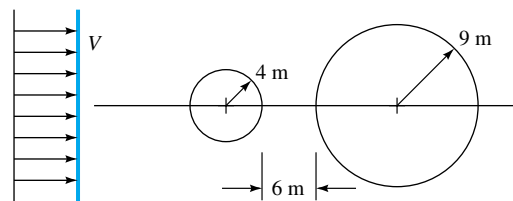


P10.4

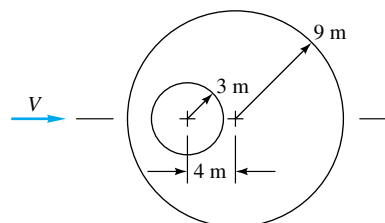
P10.5 Water flows rapidly in a channel 15 cm deep. Piercing the surface with a pencil point creates a wedgelike downstream wave of included angle 35° . Estimate the velocity V of the water.

P10.6 Pebbles dropped successively at the same point, into a water channel flow of depth 42 cm, create two circular ripples, as in Fig. P10.6. From this information estimate (a) the Froude number and (b) the stream velocity.

P10.7 Pebbles dropped successively at the same point, into a water channel flow of depth 65 cm, create two circular



P10.6



P10.7

ripples, as in Fig. P10.7. From this information estimate (a) the Froude number and (b) the stream velocity.

P10.8 An earthquake near the Kenai Peninsula, Alaska, creates a single “tidal” wave (called a *tsunami*) which propagates south across the Pacific Ocean. If the average ocean depth is 4 km and seawater density is 1025 kg/m^3 , estimate the time of arrival of this tsunami in Hilo, Hawaii.

P10.9 Equation (10.10) is for a single disturbance wave. For *periodic* small-amplitude surface waves of wavelength λ and period T , inviscid theory [5 to 9] predicts a wave propagation speed

$$c_0^2 = \frac{g\lambda}{2\pi} \tanh \frac{2\pi y}{\lambda}$$

where y is the water depth and surface tension is neglected. (a) Determine if this expression is affected by the Reynolds number, Froude number, or Weber number. Derive the limiting values of this expression for (b) $y \ll \lambda$ and (c) $y \gg \lambda$. (d) Also for what ratio y/λ is the wave speed within 1 percent of limit (c)?

P10.10 If surface tension Υ is included in the analysis of Prob. 10.9, the resulting wave speed is [5 to 9]

$$c_0^2 = \left(\frac{g\lambda}{2\pi} + \frac{2\pi\Upsilon}{\rho\lambda} \right) \tanh \frac{2\pi y}{\lambda}$$

(a) Determine if this expression is affected by the Reynolds number, Froude number, or Weber number. Derive the limiting values of this expression for (b) $y \ll \lambda$ and (c) $y \gg \lambda$. (d) Finally determine the wavelength λ_{crit} for a minimum value of c_0 , assuming that $y \gg \lambda$.

P10.11 A rectangular channel is 2 m wide and contains water 3 m deep. If the slope is 0.85° and the lining is corrugated metal, estimate the discharge for uniform flow.

- P10.12** (a) For laminar draining of a wide thin sheet of water on pavement sloped at angle θ , as in Fig. P4.36, show that the flow rate is given by

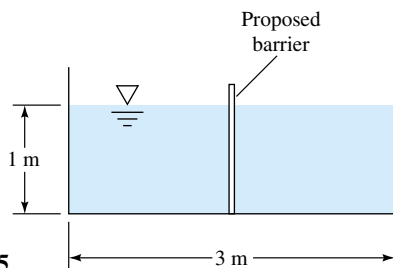
$$Q = \frac{\rho g b h^3 \sin \theta}{3\mu}$$

where b is the sheet width and h its depth. (b) By (somewhat laborious) comparison with Eq. (10.13), show that this expression is compatible with a friction factor $f = 24/Re$, where $Re = V_{av}h/\nu$.

- P10.13** The laminar-draining flow from Prob. 10.12 may undergo transition to turbulence if $Re > 500$. If the pavement slope is 0.0045, what is the maximum sheet thickness, in mm, for which laminar flow is ensured?

- P10.14** The Chézy formula (10.18) is independent of fluid density and viscosity. Does this mean that water, mercury, alcohol, and SAE 30 oil will all flow down a given open channel at the same rate? Explain.

- P10.15** The finished-concrete channel of Fig. P10.15 is designed for a flow rate of $6 \text{ m}^3/\text{s}$ at a normal depth of 1 m. Determine (a) the design slope of the channel and (b) the percentage of reduction in flow if the surface is asphalt.



- P10.16** In Prob. 10.15, for finished concrete, determine the percentage of reduction in flow if the channel is divided in the center by the proposed barrier in Fig. P10.15. How does your estimate change if all surfaces are clay tile?
- P10.17** The trapezoidal channel of Fig. P10.17 is made of brickwork and slopes at 1:500. Determine the flow rate if the normal depth is 80 cm.

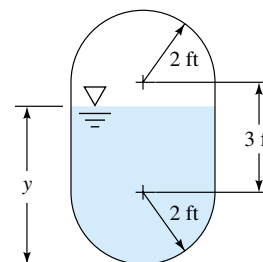


P10.17

- P10.18** Modify Prob. 10.17 as follows. Determine the normal depth for which the flow rate will be $8 \text{ m}^3/\text{s}$.
- P10.19** Modify Prob. 10.17 as follows. Let the surface be clean earth, which erodes if V exceeds 1.5 m/s. What is the maximum depth to avoid erosion?

- P10.20** A circular corrugated-metal storm drain is flowing half full over a slope 4 ft/mi. Estimate the normal discharge if the drain diameter is 8 ft.

- *P10.21** A sewer pipe has the shape of Fig. P10.21 and is constructed of unfinished concrete. The slope is 3 ft/mi. Plot the normal flow rate as a function of depth over the full range $0 < y < 7$ ft, and determine the maximum discharge and maximum velocity.



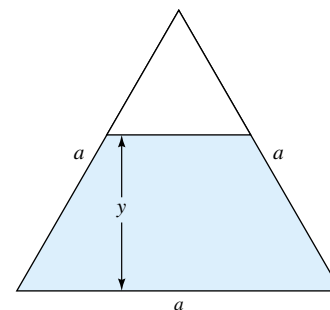
P10.21

- P10.22** A trapezoidal aqueduct (Fig. 10.7) has $b = 5$ m and $\theta = 40^\circ$ and carries a normal flow of $60 \text{ m}^3/\text{s}$ of water when $y = 3.2$ m. For clay tile surfaces, estimate the required elevation drop in m/km.

- P10.23** For the aqueduct of Prob. 10.22, if the slope is 0.0004 and the discharge is $40 \text{ m}^3/\text{s}$, use the Moody-chart formulation (10.15a) to estimate the normal depth.

- P10.24** A riveted-steel channel slopes at 1:500 and has a V shape with an included angle of 80° . Find the normal depth if the flow rate is $900 \text{ m}^3/\text{h}$.

- *P10.25** The equilateral-triangle channel in Fig. P10.25 has constant slope S_0 and constant Manning factor n . Find Q_{\max} and V_{\max} . Then, by analogy with Fig. 10.6b, plot the ratios Q/Q_{\max} and V/V_{\max} as a function of y/a for the complete range $0 < y/a < 0.866$.



P10.25

- P10.26** Water flows in a 6-m-wide rectangular channel lined with rocks whose dominant size is 20 cm. The channel slope is 0.003. Assuming uniform flow and the rock-friction correlation of Eq. (10.15b), estimate (a) the flow rate if the depth is 2 m and (b) the depth if the flow rate is

15 m³/s. (c) In part (a) what is the equivalent value of Manning's roughness factor n for the same flow rate? Does your result agree with Table 10.1?

P10.27 A circular unfinished-cement water channel has a slope of 1:600 and a diameter of 5 ft. Estimate the normal discharge in gal/min for which the average wall shear stress is 0.15 lbf/ft², and compare your result to the maximum possible discharge for this channel.

P10.28 Show that, for any straight prismatic channel in uniform flow, the average wall shear stress is given by

$$\tau_{\text{av}} \approx \rho g R_h S_0$$

If you happen to spot this result early, you can use it in solving Prob. 10.27.

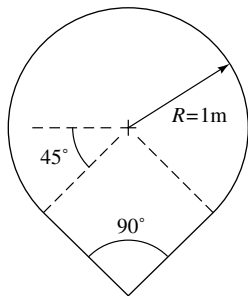
P10.29 Suppose that the trapezoidal channel of Fig. P10.17 contains sand and silt which we wish not to erode. According to an empirical correlation by A. Shields in 1936, the average wall shear stress τ_{crit} required to erode sand particles of diameter d_p is approximated by

$$\frac{\tau_{\text{crit}}}{(\rho_s - \rho)g d_p} \approx 0.5$$

where $\rho_s \approx 2400 \text{ kg/m}^3$ is the density of sand. If the slope of the channel in Fig. P10.17 is 1:900 and $n \approx 0.014$, determine the maximum water depth to keep from eroding particles of 1-mm diameter.

P10.30 A clay tile V-shaped channel, with an included angle of 90°, is 1 km long and is laid out on a 1:400 slope. When running at a depth of 2 m, the upstream end is suddenly closed while the lower end continues to drain. Assuming quasi-steady normal discharge, find the time for the channel depth to drop to 20 cm.

P10.31 A storm drain has the cross section shown in Fig. P10.31 and is laid on a slope of 1.5 m/km. If it is constructed of brickwork, find the normal discharge when it is exactly half full of water.



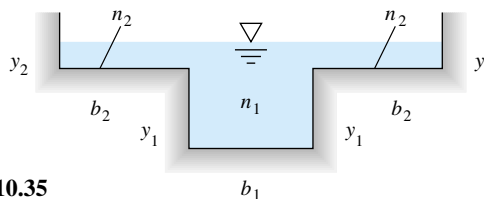
P10.31

P10.32 A 2-m-diameter clay tile sewer pipe runs half full on a slope of 0.25°. Compute the normal flow rate in gal/min.

P10.33 Five of the sewer pipes from Prob. 10.32 empty into a single asphalt pipe, also laid out at 0.25°. If the large pipe is also to run half full, what should be its diameter?

P10.34 A brick rectangular channel with $S_0 = 0.002$ is designed to carry 230 ft³/s of water in uniform flow. There is an argument over whether the channel width should be 4 or 8 ft. Which design needs fewer bricks? By what percentage?

P10.35 In flood stage a natural channel often consists of a deep main channel plus two floodplains, as in Fig. P10.35. The floodplains are often shallow and rough. If the channel has the same slope everywhere, how would you analyze this situation for the discharge? Suppose that $y_1 = 20$ ft, $y_2 = 5$ ft, $b_1 = 40$ ft, $b_2 = 100$ ft, $n_1 = 0.020$, $n_2 = 0.040$, with a slope of 0.0002. Estimate the discharge in ft³/s.



P10.35

P10.36 The Blackstone River in northern Rhode Island normally flows at about 25 m³/s and resembles Fig. P10.35 with a clean-earth center channel, $b_1 \approx 20$ m and $y_1 \approx 3$ m. The bed slope is about 2 ft/mi. The sides are heavy brush with $b_2 \approx 150$ m. During hurricane Carol in 1955, a record flow rate of 1000 m³/s was estimated. Use this information to estimate the maximum flood depth y_2 during this event.

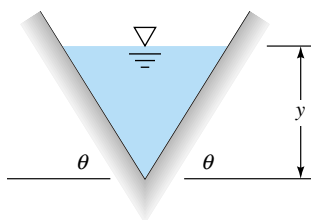
P10.37 The answer to Prob. 10.34 is that the 8-ft width is 29 percent more efficient than the 4-ft width and is almost optimum. Verify this result, using the “best-efficiency” concepts of Sec. 10.3.

P10.38 A rectangular channel has $b = 3$ m and $y = 1$ m. If n and S_0 are the same, what is the diameter of a semicircular channel that will have the same discharge? Compare the two wetted perimeters.

P10.39 A trapezoidal channel has $n = 0.022$ and $S_0 = 0.0003$ and is made in the shape of a half-hexagon for maximum efficiency. What should the length of the side of the hexagon be if the channel is to carry 225 ft³/s of water? What is the discharge of a semicircular channel of the same cross-sectional area and the same S_0 and n ?

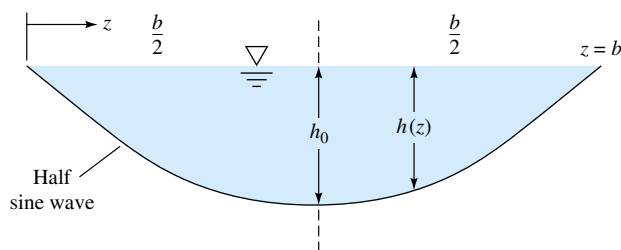
P10.40 Using the geometry of Fig. 10.6a, prove that the most efficient circular open channel (maximum hydraulic radius for a given flow area) is a semicircle.

P10.41 Determine the most efficient value of θ for the V-shaped channel of Fig. P10.41.



P10.41

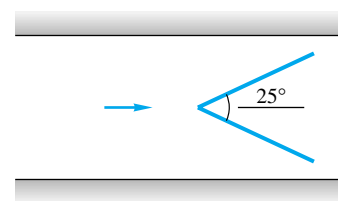
- P10.42** Suppose that the side angles of the trapezoidal channel in Prob. 10.39 are reduced to 15° to avoid earth slides. If the bottom flat width is 8 ft, (a) determine the normal depth and (b) compare the resulting wetted perimeter with the solution $P = 24.1$ ft from Prob. 10.39. (Do not reveal this answer to friends still struggling with Prob. 10.39.)
- P10.43** What are the most efficient dimensions for a riveted-steel rectangular channel to carry $4.8 \text{ m}^3/\text{s}$ at a slope of 1:900?
- P10.44** What are the most efficient dimensions for a half-hexagon cast-iron channel to carry 15,000 gal/min on a slope of 0.16°?
- P10.45** What is the most efficient depth for an asphalt trapezoidal channel, with sides sloping at 45° , to carry $3 \text{ m}^3/\text{s}$ on a slope of 0.0008?
- P10.46** It is suggested that a channel which affords minimum erosion has a half-sine-wave shape, as in Fig. P10.46. The local depth takes the form $h(z) = h_0 \sin(\pi z/b)$. For uniform-flow conditions, determine the most efficient ratio h_0/b for this channel shape.



P10.46

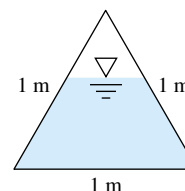
- P10.47** Replot Fig. 10.8b in the form of q versus y for constant E . Does the maximum q occur at the critical depth?
- P10.48** A wide, clean-earth river has a flow rate $q = 150 \text{ ft}^3/(\text{s} \cdot \text{ft})$. What is the critical depth? If the actual depth is 12 ft, what is the Froude number of the river? Compute the critical slope by (a) Manning's formula and (b) the Moody chart.
- P10.49** Find the critical depth of the brick channel in Prob. 10.34 for both the 4- and 8-ft widths. Are the normal flows sub- or supercritical?
- P10.50** A pencil point piercing the surface of a rectangular channel flow creates a wedgelike 25° half-angle wave, as in

Fig. P10.50. If the channel surface is painted steel and the depth is 35 cm, determine (a) the Froude number, (b) the critical depth, and (c) the critical slope for uniform flow.



P10.50

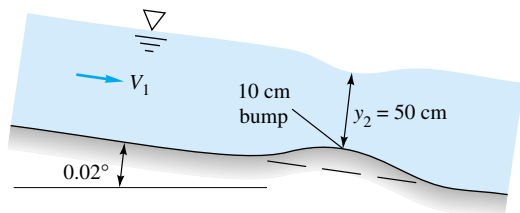
- P10.51** Modify Prob. 10.50 as follows. Let the water be flowing in an unfinished-cement half-full circular channel of diameter 60 cm. Determine (a) the Froude number, (b) the flow velocity, and (c) the critical slope.
- P10.52** Water flows full in an asphalt half-hexagon channel of bottom width W . The flow rate is $12 \text{ m}^3/\text{s}$. Estimate W if the Froude number is exactly 0.60.
- P10.53** For the river flow of Prob. 10.48, find the depth y_2 which has the same specific energy as the given depth $y_1 = 12$ ft. These are called *conjugate depths*. What is Fr_2 ?
- P10.54** A clay tile V-shaped channel has an included angle of 70° and carries $8.5 \text{ m}^3/\text{s}$. Compute (a) the critical depth, (b) the critical velocity, and (c) the critical slope for uniform flow.
- P10.55** A trapezoidal channel resembles Fig. 10.7 with $b = 1$ m and $\theta = 50^\circ$. The water depth is 2 m, and the flow rate is $32 \text{ m}^3/\text{s}$. If you stick your fingernail in the surface, as in Fig. P10.50, what half-angle wave might appear?
- P10.56** A riveted-steel triangular duct flows partly full as in Fig. P10.56. If the critical depth is 50 cm, compute (a) the critical flow rate and (b) the critical slope.



P10.56

- P10.57** For the triangular duct of Prob. 10.56, if the critical flow rate is $1.0 \text{ m}^3/\text{s}$, compute (a) the critical depth and (b) the critical slope.
- P10.58** A circular corrugated-metal channel is half full and in uniform flow at a slope $S_0 = 0.0037$. Estimate the Froude number of the flow.
- P10.59** Uniform water flow in a wide brick channel of slope 0.02° moves over a 10-cm bump as in Fig. P10.59. A slight de-

pression in the water surface results. If the minimum water depth over the bump is 50 cm, compute (a) the velocity over the bump and (b) the flow rate per meter of width.



P10.59

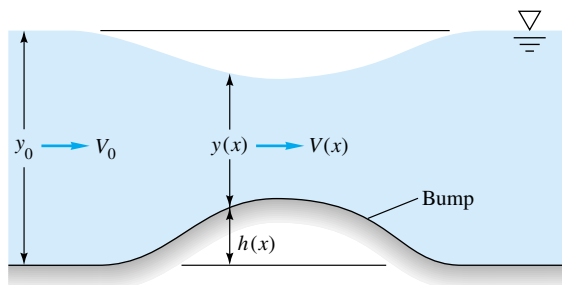
P10.60 Modify Prob. 10.59 as follows. Again assuming uniform subcritical approach flow (V_1, y_1), find (a) the flow rate and (b) y_2 for which the Froude number Fr_2 at the crest of the bump is exactly 0.8.

P10.61 Modify Prob. 10.59 as follows. Again assuming uniform subcritical approach flow (V_1, y_1), find (a) the flow rate and (b) y_2 for which the flow at the crest of the bump is exactly critical ($Fr_2 = 1.0$).

P10.62 Consider the flow in a wide channel over a bump, as in Fig. P10.62. One can estimate the water-depth change or *transition* with frictionless flow. Use continuity and the Bernoulli equation to show that

$$\frac{dy}{dx} = -\frac{dh/dx}{1 - V^2/(gy)}$$

Is the drawdown of the water surface realistic in Fig. P10.62? Explain under what conditions the surface might rise above its upstream position y_0 .



P10.62

P10.63 In Fig. P10.62 let $V_0 = 1$ m/s and $y_0 = 1$ m. If the maximum bump height is 15 cm, estimate (a) the Froude number over the top of the bump and (b) the maximum depression in the water surface.

P10.64 In Fig. P10.62 let $V_0 = 1$ m/s and $y_0 = 1$ m. If the flow over the top of the bump is exactly critical ($Fr = 1.0$), determine the bump height h_{\max} .

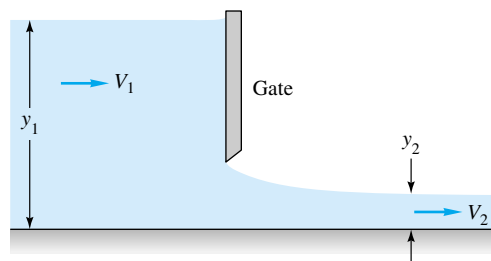
P10.65 Program and solve the differential equation of “frictionless flow over a bump,” from Prob. 10.62, for entrance conditions $V_0 = 1$ m/s and $y_0 = 1$ m. Let the bump have the convenient shape $h = 0.5h_{\max}[1 - \cos(2\pi x/L)]$, which simulates Fig. P10.62. Let $L = 3$ m, and generate a numerical solution for $y(x)$ in the bump region $0 < x < L$. If you have time for only one case, use $h_{\max} = 15$ cm (Prob. 10.63), for which the maximum Froude number is 0.425. If more time is available, it is instructive to examine a complete family of surface profiles for $h_{\max} \approx 1$ cm up to 35 cm (which is the solution of Prob. 10.64).

P10.66 In Fig. P10.62 let $V_0 = 6$ m/s and $y_0 = 1$ m. If the maximum bump height is 35 cm, estimate (a) the Froude number over the top of the bump and (b) the maximum increase in the water-surface level.

P10.67 In Fig. P10.62 let $V_0 = 6$ m/s and $y_0 = 1$ m. If the flow over the top of the bump is exactly critical ($Fr = 1.0$), determine the bump height h_{\max} .

P10.68 Modify Prob. 10.65 to have a supercritical approach condition $V_0 = 6$ m/s and $y_0 = 1$ m. If you have time for only one case, use $h_{\max} = 35$ cm (Prob. 10.66), for which the maximum Froude number is 1.47. If more time is available, it is instructive to examine a complete family of surface profiles for $1 \text{ cm} < h_{\max} < 52$ cm (which is the solution to Prob. 10.67).

***P10.69** Given is the flow of a channel of large width b under a sluice gate, as in Fig. P10.69. Assuming frictionless steady flow with negligible upstream kinetic energy, derive a formula for the dimensionless flow ratio $Q^2/(y_1^3 b^2 g)$ as a function of the ratio y_2/y_1 . Show by differentiation that the maximum flow rate occurs at $y_2 = 2y_1/3$.

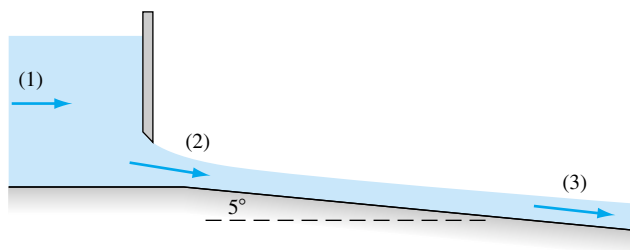


P10.69

P10.70 In Fig. P10.69 let $y_1 = 90$ cm and $V_1 = 65$ cm/s. Estimate (a) y_2 , (b) Fr_2 , and (c) the flow rate per unit width.

P10.71 In Fig. P10.69 let $y_1 = 95$ cm and $y_2 = 50$ cm. Estimate the flow rate per unit width if the upstream kinetic energy is (a) neglected and (b) included.

***P10.72** Water approaches the wide sluice gate of Fig. P10.72 at $V_1 = 0.2$ m/s and $y_1 = 1$ m. Accounting for upstream ki-


P10.72

netic energy, estimate at the outlet, section 2, the (a) depth, (b) velocity, and (c) Froude number.

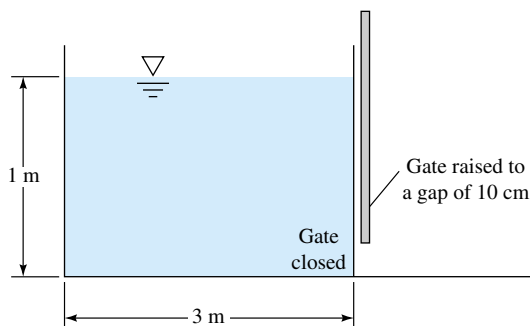
P10.73 In Fig. P10.69 suppose that $y_1 = 1.2$ m and the gate is raised so that its gap is 15 cm. Estimate the resulting flow rate per unit width.

P10.74 With respect to Fig. P10.69, show that, for frictionless flow, the upstream velocity may be related to the water levels by

$$V_1 = \sqrt{\frac{2g(y_1 - y_2)}{K^2 - 1}}$$

where $K = y_1/y_2$.

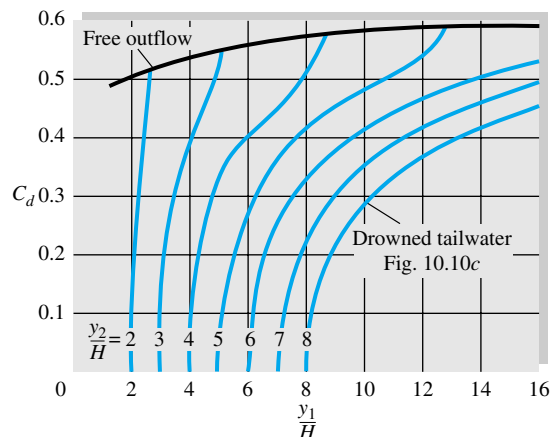
P10.75 A tank of water 1 m deep, 3 m long, and 4 m wide into the paper has a closed sluice gate on the right side, as in Fig. P10.75. At $t = 0$ the gate is opened to a gap of 10 cm. Assuming quasi-steady sluice-gate theory, estimate the time required for the water level to drop to 50 cm. Assume free outflow.


P10.75

P10.76 In Prob. 10.75 estimate what gap height would cause the tank level to drop from 1 m to 50 cm in exactly 1 min. Assume free outflow.

***P10.77** Equation (10.41) for the discharge coefficient is for free (nearly frictionless) outflow. If the outlet is *drowned*, as in Fig. 10.10c, there is dissipation and C_d drops sharply.

Figure P10.77 shows data from Ref. 3 on drowned vertical sluice gates. Use this chart to repeat Prob. 10.73, and plot the estimated flow rate versus y_2 in the range $0 < y_2 < 110$ cm.



P10.77 (From Ref. 3, p. 509.)

P10.78 Repeat Prob. 10.75 if the gate is drowned at $y_2 = 40$ cm.

P10.79 Show that the Froude number downstream of a hydraulic jump will be given by

$$Fr_2 = 8^{1/2} Fr_1 / [(1 + 8 Fr_1^2)^{1/2} - 1]^{3/2}$$

Does the formula remain correct if we reverse subscripts 1 and 2? Why?

P10.80 Water, flowing horizontally in a wide channel of depth 30 cm, undergoes a hydraulic jump whose energy dissipation is 71 percent. Estimate (a) the downstream depth and (b) the volume flow rate per meter of width.

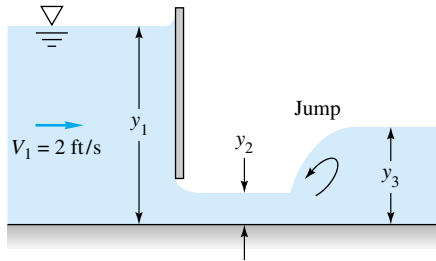
P10.81 Water flows in a wide channel at $q = 25$ ft³/(s · ft), $y_1 = 1$ ft, and then undergoes a hydraulic jump. Compute y_2 , V_2 , Fr_2 , h_f , the percentage dissipation, and the horsepower dissipated per unit width. What is the critical depth?

P10.82 The flow downstream of a wide hydraulic jump is 7 m deep and has a velocity of 2.2 m/s. Estimate the upstream (a) depth and (b) velocity and (c) the critical depth of the flow.

P10.83 A wide-channel flow undergoes a hydraulic jump from 40 to 140 cm. Estimate (a) V_1 , (b) V_2 , (c) the critical depth, in cm, and (d) the percentage of dissipation.

***P10.84** Consider the flow under the sluice gate of Fig. P10.84. If $y_1 = 10$ ft and all losses are neglected except the dissipation in the jump, calculate y_2 and y_3 and the percentage of dissipation, and sketch the flow to scale with the EGL included. The channel is horizontal and wide.

P10.85 In Prob. 10.72 the exit velocity from the sluice gate is 4.33 m/s. If there is a hydraulic jump just downstream of section 2, determine the downstream (a) velocity, (b)

**P10.84**

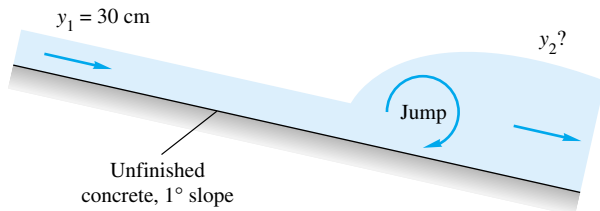
depth, (c) Froude number, and (d) percent dissipation. Neglect the effect of the nonhorizontal bottom (see Prob. 10.91).

P10.86 A bore is a hydraulic jump which propagates upstream into a still or slower-moving fluid, as in Fig. 10.4a. Suppose that the still water is 2 m deep and the water behind the bore is 3 m deep. Estimate (a) the propagation speed of the bore and (b) the induced water velocity.

P10.87 A tidal bore may occur when the ocean tide enters an estuary against an oncoming river discharge, such as on the Severn River in England. Suppose that the tidal bore is 10 ft deep and propagates at 13 mi/h upstream into a river which is 7 ft deep. Estimate the river current in kn.

P10.88 At one point in a rectangular channel 7 ft wide, the depth is 2 ft and the flow rate is 200 ft³/s. If a hydraulic jump occurs nearby, determine (a) whether it is upstream or downstream of this point and (b) the percentage of dissipation in the jump.

P10.89 Water 30 cm deep is in uniform flow down a 1° unfinished-concrete slope when a hydraulic jump occurs, as in Fig. P10.89. If the channel is very wide, estimate the water depth y_2 downstream of the jump.

**P10.89**

P10.90 Modify Prob. 10.89 as follows. Suppose that $y_2 = 1$ m and $y_1 = 30$ cm but the channel slope is not equal to 1°. Determine the proper slope for this condition.

***P10.91** No doubt you used the horizontal-jump formula (10.43) to solve Probs. 10.89 and 10.90, which is reasonable since the slope is so small. However, Chow [3, p. 425] points out that hydraulic jumps are *higher* on sloped channels, due to “the weight of the fluid in the jump.” Make a con-

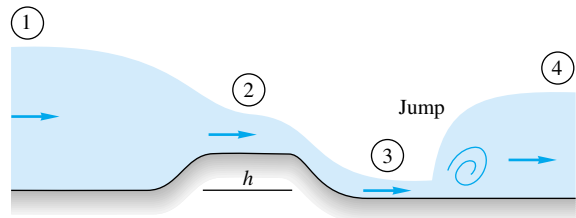
trol-volume sketch of a sloping jump to show why this is so. The sloped-jump chart given in Chow’s figure 15-20 may be approximated by the following curve fit:

$$\frac{2y_2}{y_1} \approx [(1 + 8 Fr_1^2)^{1/2} - 1]e^{3.5S_0}$$

where $0 < S_0 < 0.3$ are the channel slopes for which data are available. Use this correlation to modify your solution to Prob. 10.89. If time permits, make a graph of y_2/y_1 (≤ 20) versus Fr_1 (≤ 15) for various S_0 (≤ 0.3).

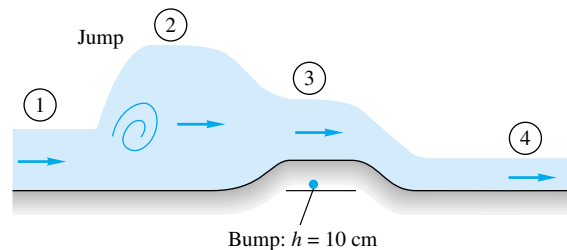
P10.92 At the bottom of an 80-ft-wide spillway is a horizontal hydraulic jump with water depths 1 ft upstream and 10 ft downstream. Estimate (a) the flow rate and (b) the horsepower dissipated.

P10.93 Water in a horizontal channel accelerates smoothly over a bump and then undergoes a hydraulic jump, as in Fig. P10.93. If $y_1 = 1$ m and $y_3 = 40$ cm, estimate (a) V_1 , (b) V_3 , (c) y_4 , and (d) the bump height h .

**P10.93**

P10.94 Modify Prob. 10.93 as follows. Let the bump height be 20 cm and the subcritical approach velocity be $V_1 = 1.5$ m/s. Determine (a) y_2 , (b) the supercritical flow V_3 , and (c) y_4 .

P10.95 A 10-cm-high bump in a wide horizontal water channel creates a hydraulic jump just upstream and the flow pattern in Fig. P10.95. Neglecting losses except in the jump, for the case $y_3 = 30$ cm, estimate (a) V_4 , (b) y_4 , (c) V_1 , and (d) y_1 .

**P10.95**

P10.96 Show that the Froude numbers on either side of a wide hydraulic jump are related by the simple relation $Fr_2 = Fr_1(y_1/y_2)^{3/2}$.

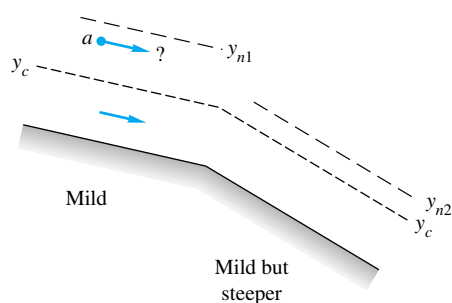
P10.97 A brickwork rectangular channel 4 m wide is flowing at $8.0 \text{ m}^3/\text{s}$ on a slope of 0.1° . Is this a mild, critical, or steep slope? What type of gradually varied solution curve are we on if the local water depth is (a) 1 m, (b) 1.5 m, and (c) 2 m?

P10.98 A gravelly earth wide channel is flowing at $10 \text{ m}^3/\text{s}$ per meter of width on a slope of 0.75° . Is this a mild, critical, or steep slope? What type of gradually varied solution curve are we on if the local water depth is (a) 1 m, (b) 2 m, and (c) 3 m?

P10.99 A clay tile V-shaped channel of included angle 60° is flowing at $1.98 \text{ m}^3/\text{s}$ on a slope of 0.33° . Is this a mild, critical, or steep slope? What type of gradually varied solution curve are we on if the local water depth is (a) 1 m, (b) 2 m, and (c) 3 m?

P10.100 If bottom friction is included in the sluice-gate flow of Prob. 10.84, the depths (y_1, y_2, y_3) will vary with x . Sketch the type and shape of gradually varied solution curve in each region (1, 2, 3), and show the regions of rapidly varied flow.

P10.101 Consider the gradual change from the profile beginning at point a in Fig. P10.101 on a mild slope S_{01} to a mild but steeper slope S_{02} downstream. Sketch and label the curve $y(x)$ expected.



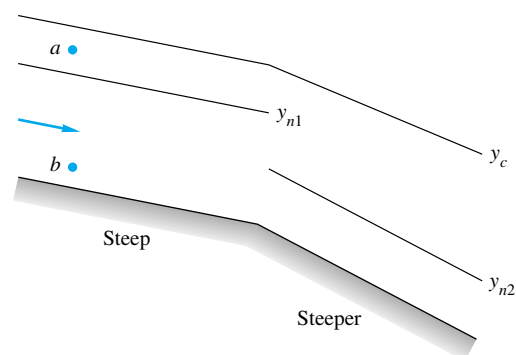
P10.101

***P10.102** The wide-channel flow in Fig. P10.102 changes from a steep slope to one even steeper. Beginning at points a and b , sketch and label the water-surface profiles which are expected for gradually varied flow.

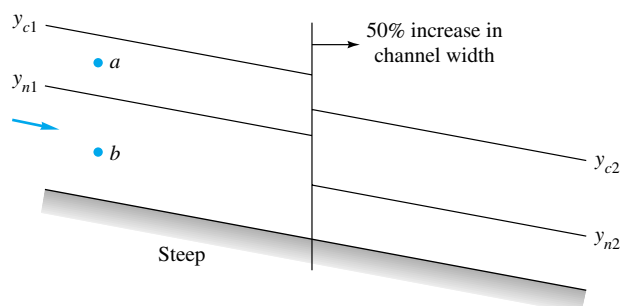
P10.103 A circular painted-steel channel is running half full at $1 \text{ m}^3/\text{s}$ and is laid out on a slope of 5 m/km. Is this a mild or steep slope, of type 1, 2, or 3? Take $R = 50 \text{ cm}$.

P10.104 The rectangular-channel flow in Fig. P10.104 expands to a cross section 50 percent wider. Beginning at points a and b , sketch and label the water-surface profiles which are expected for gradually varied flow.

P10.105 In Prob. 10.84 the frictionless solution is $y_2 = 0.82 \text{ ft}$, which we denote as $x = 0$ just downstream of the gate. If the channel is horizontal with $n = 0.018$ and there is



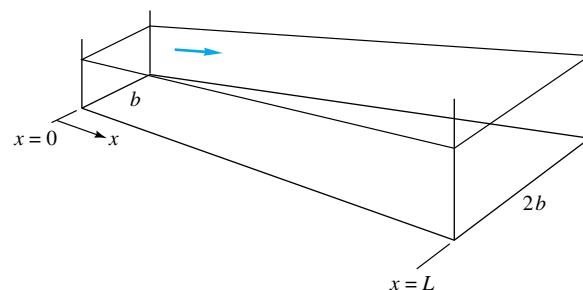
P10.102



P10.104

no hydraulic jump, compute from gradually varied theory the downstream distance where $y = 2.0 \text{ ft}$.

P10.106  A rectangular channel with $n = 0.018$ and a constant slope of 0.0025 increases its width linearly from b to $2b$ over a distance L , as in Fig. P10.106. (a) Determine the variation $y(x)$ along the channel if $b = 4 \text{ m}$, $L = 250 \text{ m}$, the initial depth is $y(0) = 1.05 \text{ m}$, and the flow rate is $7 \text{ m}^3/\text{s}$. (b) Then, if your computer program is running well, determine the initial depth $y(0)$ for which the exit flow will be exactly critical.

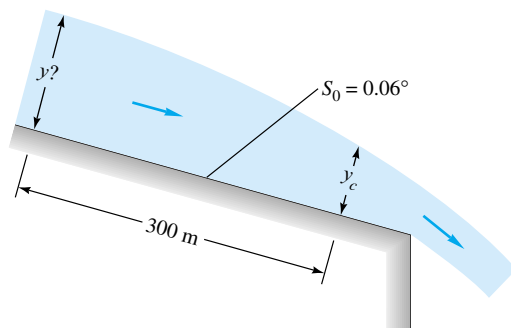


P10.106

P10.107 A clean-earth wide-channel flow is flowing up an adverse slope with $S_0 = -0.002$. If the flow rate is $q = 4.5 \text{ m}^3/(\text{s} \cdot \text{m})$, use gradually varied theory to compute the distance for the depth to drop from 3.0 to 2.0 m.

P10.108 Illustrate Prob. 10.104 with a numerical example. Let the channel be rectangular with a width $b_1 = 10 \text{ m}$ for $0 < x < 100 \text{ m}$, expanding to $b_2 = 15 \text{ m}$ for $100 < x < 250 \text{ m}$. The flow rate is $27 \text{ m}^3/\text{s}$, and $n = 0.012$. Compute the water depth at $x = 250 \text{ m}$ for initial depth $y(0)$ equal to (a) 75 cm and (b) 5 cm. Compare your results with the discussion in Prob. 10.104. Let $S_0 = 0.005$.

P10.109 Figure P10.109 illustrates a free overfall or *dropdown* flow pattern, where a channel flow accelerates down a slope and falls freely over an abrupt edge. As shown, the flow reaches critical just before the overfall. Between y_c and the edge the flow is rapidly varied and does not satisfy gradually varied theory. Suppose that the flow rate is $q = 1.3 \text{ m}^3/(\text{s} \cdot \text{m})$ and the surface is unfinished cement. Use Eq. (10.51) to estimate the water depth 300 m upstream as shown.

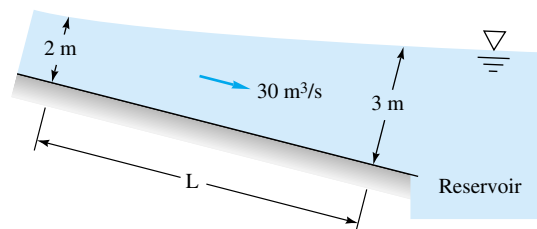


P10.109

P10.110 We assumed frictionless flow in solving the bump case, Prob. 10.65, for which $V_2 = 1.21 \text{ m/s}$ and $y_2 = 0.826 \text{ m}$ over the crest when $h_{\max} = 15 \text{ cm}$, $V_1 = 1 \text{ m/s}$, and $y_1 = 1 \text{ m}$. However, if the bump is long and rough, friction may be important. Repeat Prob. 10.65 for the same bump shape, $h = 0.5h_{\max}[1 - \cos(2\pi x/L)]$, to compute conditions (a) at the crest and (b) at the end of the bump, $x = L$. Let $h_{\max} = 15 \text{ cm}$ and $L = 100 \text{ m}$, and assume a clean-earth surface.

P10.111 Modify Prob. 10.110 as follows. Keep all other data the same, and find the bump length L for which the flow first becomes critical somewhere along the bump surface.

P10.112 The clean-earth channel in Fig. P10.112 is 6 m wide and slopes at 0.3° . Water flows at $30 \text{ m}^3/\text{s}$ in the channel and enters a reservoir so that the channel depth is 3 m just before the entry. Assuming gradually varied flow, how far is the distance L to a point in the channel where $y = 2 \text{ m}$? What type of curve is the water surface?

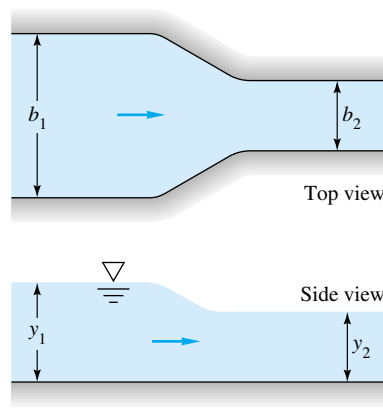


P10.112

P10.113 Figure P10.113 shows a channel contraction section often called a *venturi flume* [19, p. 167], because measurements of y_1 and y_2 can be used to meter the flow rate. Show that if losses are neglected and the flow is one-dimensional and subcritical, the flow rate is given by

$$Q = \left[\frac{2g(y_1 - y_2)}{1/(b_2^2 y_2^3) - 1/(b_1^2 y_1^3)} \right]^{1/2}$$

Apply this to the special case $b_1 = 3 \text{ m}$, $b_2 = 2 \text{ m}$, and $y_1 = 1.9 \text{ m}$. (a) Find the flow rate if $y_2 = 1.5 \text{ m}$. (b) Also find the depth y_2 for which the flow becomes critical in the throat.



P10.113

P10.114 Investigate the possibility of *choking* in the venturi flume of Fig. P10.113. Let $b_1 = 4 \text{ ft}$, $b_2 = 3 \text{ ft}$, and $y_1 = 2 \text{ ft}$. Compute the values of y_2 and V_1 for a flow rate of (a) $30 \text{ ft}^3/\text{s}$ and (b) $35 \text{ ft}^3/\text{s}$. Explain your vexation.

P10.115 Gradually varied theory, Eq. (10.49), neglects the effect of *width* changes, db/dx , assuming that they are small. But they are not small for a short, sharp contraction such as the venturi flume in Fig. P10.113. Show that, for a rectangular section with $b = b(x)$, Eq. (10.49) should be modified as follows:

$$\frac{dy}{dx} \approx \frac{S_0 - S + [V^2/(gb)](db/dx)}{1 - \text{Fr}^2}$$

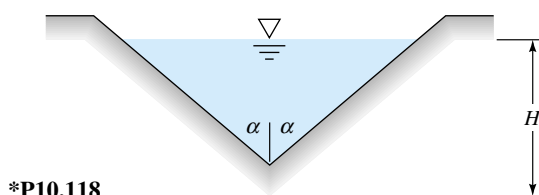
Investigate a criterion for reducing this relation to Eq. (10.49).

- P10.116** Investigate the possibility of *frictional effects* in the venturi flume of Prob. 10.113, part (a), for which the frictionless solution is $Q = 9.88 \text{ m}^3/\text{s}$. Let the contraction be 3 m long and the measurements of y_1 and y_2 be at positions 3 m upstream and 3 m downstream of the contraction, respectively. Use the modified gradually varied theory of Prob. 10.115, with $n = 0.018$ to estimate the flow rate.

- P10.117** A full-width weir in a horizontal channel is 5 m wide and 80 cm high. The upstream depth is 1.5 m. Estimate the flow rate for (a) a sharp-crested weir and (b) a rounded broad-crested weir.

- *P10.118** Using a Bernoulli-type analysis similar to Fig. 10.16a, show that the theoretical discharge of the V-shaped weir in Fig. P10.118 is given by

$$Q = 0.7542g^{1/2} \tan \alpha H^{5/2}$$



***P10.118**

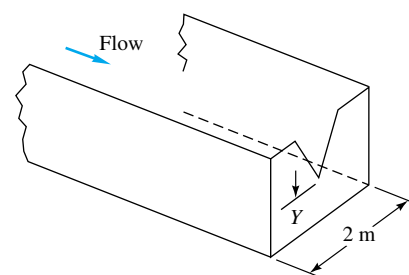
- P10.119** Data by A. T. Lenz for water at 20°C (reported in Ref. 19) show a significant increase of discharge coefficient of V-notch weirs (Fig. P10.118) at low heads. For $\alpha = 20^\circ$, some measured values are as follows:

H , ft	0.2	0.4	0.6	0.8	1.0
C_d	0.499	0.470	0.461	0.456	0.452

Determine if these data can be correlated with the Reynolds and Weber numbers vis-à-vis Eq. (10.61). If not, suggest another correlation.

- P10.120** The rectangular channel in Fig. P10.120 contains a V-notch weir as shown. The intent is to meter flow rates between 2.0 and 6.0 m^3/s with an upstream hook gage set to measure water depths between 2.0 and 2.75 m. What are the most appropriate values for the notch height Y and the notch half-angle α ?

- P10.121** Water flow in a rectangular channel is to be metered by a thin-plate weir with side contractions, as in Table 10.1b, with $L = 6 \text{ ft}$ and $Y = 1 \text{ ft}$. It is desired to measure flow rates between 1500 and 3000 gal/min with only a 6-in change in upstream water depth. What is the most appropriate length for the weir width b ?



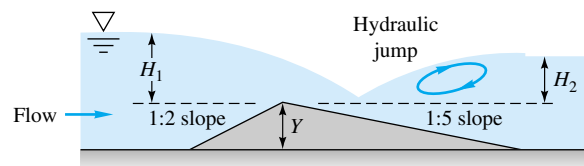
P10.120

- P10.122** In 1952 E. S. Crump developed the triangular weir shape shown in Fig. P10.122 [19, chap. 4]. The front slope is 1:2 to avoid sediment deposition, and the rear slope is 1:5 to maintain a stable tailwater flow. The beauty of the design is that it has a unique discharge correlation up to near-drowning conditions, $H_2/H_1 \leq 0.75$:

$$Q = C_d b g^{1/2} \left(H_1 + \frac{V_1^2}{2g} - k_h \right)^{3/2}$$

where $C_d \approx 0.63$ and $k_h \approx 0.3 \text{ mm}$

The term k_h is a low-head loss factor. Suppose that the weir is 3 m wide and has a crest height $Y = 50 \text{ cm}$. If the water depth upstream is 65 cm, estimate the flow rate in gal/min.



P10.122 The Crump weir [19, chap. 4]

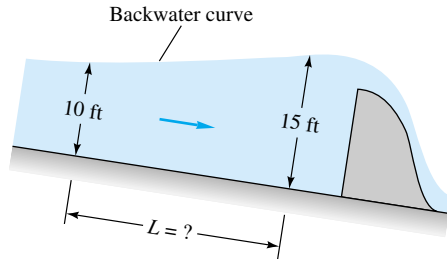
- *P10.123** The Crump weir calibration in Prob. 10.122 is for *modular* flow, i.e., when the flow rate is independent of downstream tailwater. When the weir becomes drowned, the flow rate decreases by the following factor:

$$Q = Q_{\text{mod}} f$$

where $f \approx 1.035 \left[0.817 - \left(\frac{H_2^*}{H_1^*} \right)^4 \right]^{0.0647}$

for $0.70 \leq H_2^*/H_1^* \leq 0.93$, where H^* denotes $H_1 + V_1^2/(2g) - k_h$ for brevity. The weir is then *double-gaged* to measure both H_1 and H_2 . Suppose that the weir crest is 1 m high and 2 m wide. If the measured upstream and downstream water depths are 2.0 and 1.9 m, respectively, estimate the flow rate in gal/min. Comment on the possible uncertainty of your estimate.

- P10.124** Water flows at $600 \text{ ft}^3/\text{s}$ in a rectangular channel 22 ft wide with $n \approx 0.024$ and a slope of 0.1° . A dam increases the depth to 15 ft, as in Fig. P10.124. Using gradually varied theory, estimate the distance L upstream at which the water depth will be 10 ft. What type of solution curve are we on? What should be the water depth asymptotically far upstream?

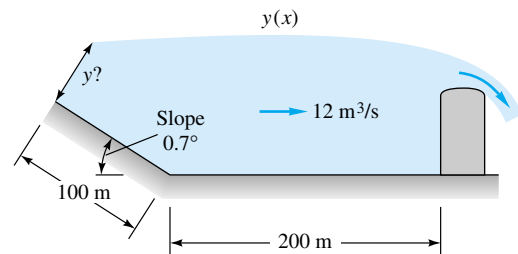
**P10.124**

- P10.125** The Tupperware dam on the Blackstone River is 12 ft high, 100 ft wide, and sharp-edged. It creates a backwater similar to Fig. P10.124. Assume that the river is a weedy-earth rectangular channel 100 ft wide with a flow rate of $800 \text{ ft}^3/\text{s}$. Estimate the water-depth 2 mi upstream of the dam if $S_0 = 0.001$.
- P10.126** Suppose that the rectangular channel of Fig. P10.120 is made of riveted steel and carries a flow of $8 \text{ m}^3/\text{s}$ on a

slope of 0.15° . If the V-notch weir has $\alpha = 30^\circ$ and $Y = 50 \text{ cm}$, estimate, from gradually varied theory, the water depth 100 m upstream.

- P10.127** A horizontal gravelly earth channel 2 m wide contains a full-width Crump weir (Fig. P10.122) 1 m high. If the weir is not drowned, estimate, from gradually varied theory, the flow rate for which the water depth 100 m upstream will be 2 m.

- P10.128** A rectangular channel 4 m wide is blocked by a broad-crested weir 2 m high, as in Fig. P10.128. The channel is horizontal for 200 m upstream and then slopes at 0.7° as shown. The flow rate is $12 \text{ m}^3/\text{s}$, and $n = 0.03$. Compute the water depth y at 300 m upstream from gradually varied theory.

**P10.128****Word Problems**

- W10.1** Free-surface problems are driven by gravity. Why do so many of the formulas in this chapter contain the *square root* of the acceleration of gravity?
- W10.2** Explain why the flow under a sluice gate, Fig. 10.10, either is or is not analogous to compressible gas flow through a converging-diverging nozzle, Fig. 9.12.
- W10.3** In uniform open-channel flow, what is the balance of forces? Can you use such a force balance to derive the Chézy equation (10.13)?
- W10.4** A shallow-water wave propagates at the speed $c_0 \approx (gy)^{1/2}$. What makes it propagate? That is, what is the balance of forces in such wave motion? In which direction does such a wave propagate?
- W10.5** Why is the Manning friction correlation, Eq. (10.16), used almost universally by hydraulics engineers, instead of the Moody friction factor?
- W10.6** During horizontal channel flow over a bump, is the specific energy constant? Explain.
- W10.7** Cite some similarities, and perhaps some dissimilarities, between a hydraulic jump and a gas-dynamic normal-shock wave.
- W10.8** Give three examples of rapidly varied flow. For each case, cite reasons why it does not satisfy one or more of the five basic assumptions of gradually varied flow theory.
- W10.9** Is a free overfall, Fig. 10.15e, similar to a weir? Could it be calibrated versus flow rate in the same manner as a weir? Explain.
- W10.10** Cite some similarities, and perhaps some dissimilarities, between a weir and a Bernoulli obstruction flowmeter from Sec. 6.7.
- W10.11** Is a bump, Fig. 10.9a, similar to a weir? If not, when does a bump become large enough, or sharp enough, to be a weir?
- W10.12** After doing some reading and/or thinking, explain the design and operation of a *long-throated flume*.
- W10.13** Describe the design and operation of a *critical-depth flume*. What are its advantages compared to the venturi flume of Prob. 10.113?

Fundamentals of Engineering Exam Problems

The FE Exam is fairly light on open-channel problems in the general (morning) session, but it plays a big part in the specialized civil engineering (afternoon) exam.

- FE10.1** Consider a rectangular channel 3 m wide laid on a 1° slope. If the water depth is 2 m, the hydraulic radius is (a) 0.43 m, (b) 0.6 m, (c) 0.86 m, (d) 1.0 m, (e) 1.2 m
- FE10.2** For the channel of Prob. FE10.1, the most efficient water depth (best flow for a given slope and resistance) is (a) 1 m, (b) 1.5 m, (c) 2 m, (d) 2.5 m, (e) 3 m
- FE10.3** If the channel of Prob. FE10.1 is built of rubble cement (Manning's $n \approx 0.020$), what is the uniform-flow rate when the water depth is 2 m?
(a) $6 \text{ m}^3/\text{s}$, (b) $18 \text{ m}^3/\text{s}$, (c) $36 \text{ m}^3/\text{s}$, (d) $40 \text{ m}^3/\text{s}$, (e) $53 \text{ m}^3/\text{s}$
- FE10.4** For the channel of Prob. FE10.1, if the water depth is 2 m and the uniform-flow rate is $24 \text{ m}^3/\text{s}$, what is the approximate value of Manning's roughness factor n ?
(a) 0.015, (b) 0.020, (c) 0.025, (d) 0.030, (e) 0.035
- FE10.5** For the channel of Prob. FE10.1, if Manning's roughness factor $n \approx 0.020$ and $Q \approx 29 \text{ m}^3/\text{s}$, what is the normal depth y_n ?
(a) 1 m, (b) 1.5 m, (c) 2 m, (d) 2.5 m, (e) 3 m
- FE10.6** For the channel of Prob. FE10.1, if $Q \approx 24 \text{ m}^3/\text{s}$, what is the critical depth y_c ?
(a) 1.0 m, (b) 1.26 m, (c) 1.5 m, (d) 1.87 m, (e) 2.0 m
- FE10.7** For the channel of Prob. FE10.1, if $Q \approx 24 \text{ m}^3/\text{s}$ and the depth is 2 m, what is the Froude number of the flow?
(a) 0.50, (b) 0.77, (c) 0.90, (d) 1.00, (e) 1.11

Comprehensive Problems

- C10.1** February 1998 saw the failure of the earthen dam impounding California Jim's Pond in southern Rhode Island. The resulting flood raised temporary havoc in the nearby village of Peace Dale. The pond is 17 acres in area and 15 ft deep and was full from heavy rains. The breach in the dam was 22 ft wide and 15 ft deep. Estimate the time required for the pond to drain to a depth of 2 ft.
- C10.2** A circular, unfinished concrete drainpipe is laid on a slope of 0.0025 and is planned to carry from 50 to $300 \text{ ft}^3/\text{s}$ of runoff water. Design constraints are that (1) the water depth should be no more than three-fourths of the diameter and (2) the flow should always be subcritical. What is the appropriate pipe diameter to satisfy these requirements? If no commercial pipe is exactly this calculated size, should you buy the next smallest or the next largest pipe?
- C10.3** Extend Prob. 10.72, whose solution was $V_2 \approx 4.33 \text{ m/s}$. Use gradually varied theory to estimate the water depth 10 m downstream at section (3) for (a) the 5° unfinished-concrete slope shown in Fig. P10.72. (b) Repeat your calculation for an upward (adverse) slope of 5° . (c) When you find that part (b) is impossible with gradually varied theory, explain why and repeat for an adverse slope of 1° .

Design Projects

- D10.1** A straight weedy-earth channel has the trapezoidal shape of Fig. 10.7, with $b = 4 \text{ m}$ and $\theta = 35^\circ$. The channel has a constant bottom slope of 0.001. The flow rate varies seasonally from 5 up to $10 \text{ m}^3/\text{s}$. It is desired to place a sharp-edged weir across the channel so that the water depth 1 km upstream remains at $2.0 \text{ m} \pm 10$ percent throughout the year. Investigate the possibility of accomplishing this with a full-width weir; if successful, determine the proper weir height Y . If unsuccessful, try other alternatives, such as (a) a full-width broad crested weir or (b) a weir with side contractions or (c) a V-notch weir. Whatever your final design, cite the seasonal variation of normal depths and critical depths for comparison with the desired year-round depth of 2 m.
- D10.2** The Caroselli Dam on the Pawcatuck River is 10 ft high, 90 ft wide, and sharp edged. The Coakley Company uses this head to generate hydropower electricity and wants more head. They ask the town for permission to raise the dam higher. The river above the dam may be approximated as rectangular, 90 ft wide, sloping upstream at 12 ft per statute mile, and with a stony, cobbled bed. The average flow rate is $400 \text{ ft}^3/\text{s}$, with a 30-year predicted flood rate of $1200 \text{ ft}^3/\text{s}$. The river sides are steep until 1 mi upstream, where there are low-lying residences. The town council agrees the dam may be heightened if the new river level near these houses, during the 30-year flood, is no more than 3 ft higher than the present level during average-flow conditions. You, as project engineer, have to predict how high the dam crest can be raised and still meet this requirement.

References

1. R. H. French, *Open-Channel Hydraulics*, McGraw-Hill, New York, 1985.
2. M. H. Chaudhry, *Open Channel Flow*, Prentice-Hall, Upper Saddle River, NJ, 1993.
3. Ven Te Chow, *Open Channel Hydraulics*, McGraw-Hill, New York, 1959.
4. F. M. Henderson, *Open Channel Flow*, Macmillan, New York, 1966.
5. B. Kinsman, *Wind Waves: Their Generation and Propagation on the Ocean Surface*, Prentice-Hall, Englewood Cliffs, NJ, 1964; Dover, New York, 1984.
6. M. J. Lighthill, *Waves in Fluids*, Cambridge University Press, London, 1978.
7. C. C. Mei, *The Applied Dynamics of Ocean Surface Waves*, Wiley, New York, 1983.
8. A. T. Ippen, *Estuary and Coastline Hydrodynamics*, McGraw-Hill, New York, 1966.
9. R. M. Sorenson, *Basic Coastal Engineering*, Wiley, New York, 1978.
10. J. M. Robertson and H. Rouse, "The Four Regimes of Open Channel Flow," *Civ. Eng.*, vol. 11, no. 3, March 1941, pp. 169–171.
11. R. W. Powell, "Resistance to Flow in Rough Channels," *Trans. Am. Geophys. Union*, vol. 31, no. 4, August 1950, pp. 575–582.
12. R. Manning, "On the Flow of Water in Open Channels and Pipes," *Trans. I.C.E. Ireland*, vol. 20, 1891, pp. 161–207.
13. B. A. Bakhmeteff, *Hydraulics of Open Channels*, McGraw-Hill, New York, 1932.
14. P. A. Thompson, *Compressible-Fluid Dynamics*, McGraw-Hill, New York, 1972.
15. E. F. Brater, *Handbook of Hydraulics*, 6th ed., McGraw-Hill, New York, 1976.
16. U.S. Bureau of Reclamation, "Research Studies on Stilling Basins, Energy Dissipators, and Associated Appurtenances," *Hydraulic Lab. Rep. Hyd-399*, June 1, 1955.
17. "Friction Factors in Open Channels, Report of the Committee on Hydromechanics," *ASCE J. Hydraul. Div.*, March 1963, pp. 97–143.
18. R. M. Olson and S. J. Wright, *Essentials of Engineering Fluid Mechanics*, 5th ed., Harper & Row, New York, 1990.
19. P. Ackers et al., *Weirs and Flumes for Flow Measurement*, Wiley, New York, 1978.
20. M. G. Bos, J. A. Replogle, and A. J. Clemmens, *Flow Measuring Flumes for Open Channel Systems*, Wiley, New York, 1984.
21. M. G. Bos, *Long-Throated Flumes and Broad-Crested Weirs*, Martinus Nijhoff (Kluwer), Dordrecht, The Netherlands, 1985.
22. U.S. Army Corps of Engineers, *HEC-2 Water Surface Profiles*, Hydrologic Engineering Center, 609 Second Street, Davis, CA.
23. W. Rodi, *Turbulence Models and Their Application in Hydraulics*, Brookfield Publishing, Brookfield, VT, 1984.